Lawrence Berkeley National Laboratory
Lawrence Berkeley National Laboratory

Title
CALCULATIONS OF THE ELECTRON DAMPING FORCE ON MOVING EDGE DISLOCATIONS

Permalink
https://escholarship.org/uc/item/88q810g8

Author
Mohri, T.

Publication Date
1982-11-01

Peer reviewed

eScholarship.org Powered by the California Digital Library
University of California

LBL--12223

DE83 011744

CALCULATIONS OF THE ELECTRON-DAMPING FORCE ON MOVING-EDGE DISLOCATIONS

Tetsuo Mohri

Materials and Molecular Research Division,

Lawrence Berkeley Laboratory

and

Department of Materials Science and Mineral Engineering,

University of California, Berkeley, California 94720

NOTICE
PORTIONS OF THIS REPORT ARE ILLEGIBLE.
It has been reproduced from the best available copy to permit the broadest possible availability.

ABSTRACT

Dynamic effect of a moving dislocation has been recognized as one of essential features of deformation behavior at very low temperatures. Damping mechanisms are the central problems in this field. Based on the free-electron-gas model, the electron-damping force (friction force) on a moving-edge dislocation in a normal state is estimated. By applying classical Mackenzie-Sondheimer's procedures, the electrical resistivity caused by a moving dislocation is first estimated, and the damping force is calculated as a Joule-heat-energy dissipation. The calculated values are 3.63×10^{-6},

This manuscript was printed from originals provided by the author.

DISTRIBUTION OF THIS DOCUMENT IS UNLIMITED

7.62×10^{-7} and 1.00×10^{-6} $[dyn\cdot sec/cm^{-2}]$ for Al, Cu and Pb, respectively. These values show fairly good agreements as compared with experimental results. Also, numerical calculations are carried out to estimate magnetic effects caused by a moving dislocation. The results are negative and any magnetic effects are not expected.

In order to treat deformation behavior at very low temperatures, a unification of three important deformation problems is attempted and a fundamental equation is derived.

ACKNOWLEDGEMENTS

My sincere thanks to Professor J. W. Morris, Jr. for his guidance and support throughout the course of this work, and to Professors D. de Fontaine and Ole H. Hald for their reviewing this manuscript. Special thanks to Dr. Warren Garrison, Jr. for his reviewing this manuscript, and to Mr. Gianni Fior for his computer assistence, as well as for their friendships.

I would like to acknowledge the staff and faculty in both the Hearst Mining Building and M.M.R.D. of the Lawrence Berkeley Laboratory, especially Mrs. Jeanne Shull and Gloria Pelatowski.

Thanks is due to Professor and Mrs. Leo Kanowitz for their continuous encouragement and enlightenment throughout my life here in United States.

Finally I would like to thank my family especially my parents and my wife, Fumiko, for their encouragement, support and everything.

This work was supported by the Director, Office of Energy Research, Office of Basic Energy Sciences, Materials Sciences Division of the U. S. Department of Energy under contract No. DE-AC03-76SF00098.

DISCLAIMER

This report was prepared as an account of work sponsored by an agency of the United States Government. Neither the United States Government nor any agency thereof, nor any of their employees, makes any warranty, express or implied, or assumes any legal liability or responsibility for the accuracy, completeness, or usefulness of any information, apparatus, product, or process disclosed, or represents that its use would not infringe privately owned rights. Reference herein to any specific commercial product, process, or service by trade name, trademark, manufacturer, or otherwise does not necessarily constitute or imply its endorsement, recommendation, or favoring by the United States Government or any agency thereof. The views and opinions of authors expressed herein do not necessarily state or reflect those of the United States Government or any agency thereof.

TABLE OF CONTENTS

I. INTRODUCTION

I-1. General Characterization of Theoretical Problems of Dislocation Behavior

Various properties of materials, optical, electrical, chemical, mechanical, etc., are more or less influenced by dislocations. Especially, the mechanical properties of metals and alloys which are central concerns of physical metallurgy are largely determined by dislocation behavior. Although significant progress in dislocation theory has been made, the basic understanding of physical properties of dislocations is still insufficient to supply a useful guide lines for alloy design. A general characterization of the important problems in dislocation theory based on the author's point of view is summarized below.

It is well known that the dislocation density of a well annealed metal is approximately $10^6 cm^{-2}$ and that of a deformed metal is approximately $10^{12} cm^{-2}$ which is 250 times as long as our equator length. These tremendous amounts of dislocations are often observed to interact in a very complicated manner and to tangle one another. However complicated their configurations and interactions might be, since plastic deformation is a natural phenomena the group behavior of these dislocations must be strictly obeyed by certain physical principles or natural laws. The search for such a physical principle known as the "collective behavior of dislocations" or "multiple behavior of dislocations" is considered to be an extremely important problem in a analysis of macroscopic mechanical behavior. Although the theory has been mostly devoted to single dislocation behavior no one can really understand and predict macroscopic crystal plasticity without the knowledge of the collective behavior of dislocations. A key factor of this problem is the development of a suitable thermodynamical treatment.

Apart from the many body problems of dislocation theory mentioned

above, the behavior of single dislocations is of fundamental importance. This problem can be split into two sub-categories.

One is the "elementary interaction process" which deals with interaction process between single dislocations and various types of obstacles such as solute atoms, 2nd phase, other dislocations and so on. This problem, the main concern of this thesis, is discussed in detail in the next section.

The other category is characterized as a statistical aspect of a dislocation behavior. Critical resolved shear stress (c.r.s.s.) can not be uniquely determined even if the elementary interaction process between a dislocation and a obstacle is well established. This is because c.r.s.s. is not a simple sum of each resistance force caused by obstacles but complicated function of the distributions, concentrations and strength spectrums etc. of obstacles which are scattered on a slip plane and of the line tension of a dislocation. Direct computer simulation techniques have been most successfully applied to this statistical problem and analytical calculations based on geometrical consideration or functional analysis were examined.

Attentions should be paid equally to these three categories in order to fully understand dislocation behavior and to develop a dislocation theory of power sufficient to provide realistic criteria for the design of new alloys. This study is, however, focussed on the elementary interaction process and the details of this problem are introduced in the next section.

I-2. Elementary Interaction Process

Since the first theoretical prediction of the existence of a dislocation line by Ewing et.al. in 1899 [1] most theoretical efforts have been concentrated on the problem of how to explain macroscopically observed strength in terms of microscopic dislocation interactions with various types of obstacles. Typical

examples are found in studies of solid solution hardening and dispersion hardening effects. These calculations are based on continuum elasticity theory and a static equilibrium configuration between a dislocation and a obstacle is assumed. Furthermore, rate processes have been described within a frame of absolute rate theory of Eyring.

However, with the progress of low temperature measurement techniques in this fifteen years, various types of abnormal deformation behavior which can not be explained by simple extrapolation of high temperature deformation mechanisms have been reported. The sudden change of flow stress of a lead polycrystal due to the transition between the normal and superconducting states measured by Suzuki et.al.[2] and Pustovalov et.al [3] in 1968, or the abrupt drop in the temperature dependence of the yield stress of Cu and its dilute alloys below 50^0 K found by Kamata et.al.[4] are typical examples of those anomalies. Since, at present, it is still difficult to extend the in-situ TEM technique to low temperatures and to observe a dislocation behavior directly, one should neither jump at the conclusion nor ascribe these anomalies to a single cause. But, by comparing the results of different experimental approaches, the dynamic interaction of dislocations with "microscopic obstacles" such as phonons, electrons etc. has been recognized as most plausible source of these anomalies. Especially, in f.c.c. metals of which Peierls potential is relatively small, the dominant mode of dislocation motion is free flight motion (spurt-like motion) and dislocation velocities of up to $10^{2\sim3}$ cm/sec [5] have been measured in Cu even at room temperature. These facts might quite naturally lead one to the idea of a dynamic effect.

Mathematically the anomalies mentioned above can be re-explained in the following way. According to the string model of a dislocation which was originally introduced by Koehler [6] the motion equation can be written as

$$m_d \frac{\partial^2 y}{\partial t^2} + B\frac{\partial y}{\partial t} + \Gamma\frac{\partial^2 y}{\partial x^2} + \tau_{eff} b = 0 \qquad (1\text{-}1)$$

where m_d is the mass of a dislocation per unit length, B is a damping constant caused by electrons or phonons etc., Γ is the line tension, b is the magnitude of the Burgers vector, (x,y) is the coordinate system on the active slip plane, t is time and τ_{eff} is the effective stress on the dislocation line. This effective stress is explicitly given by

$$\tau_{eff} = \tau_{app} - \tau_i(x,y) \qquad (1\text{-}2)$$

where τ_{app} is the applied stress and $\tau_i(x,y)$ is the internal stress caused by obstacles.

Therefore eq.1-1 is the force balance condition among inertia force, damping force, line tension and effective applied stress on a dislocation. In earlier treatments, the last two terms were sufficient enough to describe the static equilibrium condition, and primary interest was the functional form of the internal stress, $\tau_i(x,y)$, including its spatial distribution, strength spectrum etc.. However, abnormal plasticity of low temperatures implies two additional dynamic terms, namely inertia force and damping force. These additional terms will force one to reexamine the statistical problem mentioned in the former section and will not permit the rate process to be described by simple absolute rate theory of Eyring. Especially, the latter problem, how to combine thermally activated processes with kinetics, poses tremendous difficulties and can not be resolved without returning the fundamental physics.

The main object of this study is the investigation of the physical origin of the "microscopic interaction", namely damping, and the estimation of the magnitude of this damping force.

I-3. Damping Force

There are many damping mechanisms for a dislocation. Among them, the following three mechanisms are important. They are phonon damping, electron damping and reradiation damping. Therefore the damping constant, B, in the eq. 1-1 is rewritten as

$$B = B_p + B_e + B_r \tag{1-3}$$

Phonon damping can be further divided into two mechanisms. One is phonon scattering of which the main process is the scattering of phonons by the dislocation strain field, and the other is phonon viscosity which involves the separation of the effective temperatures of different phonon modes produced by the shear stress field of the moving dislocation and its relaxation to equilibrium, which was proposed by Mason [7]. Phonon damping has been revealed to be monotonically increasing with temperature, and in the case of very low temperatures where the lattice vibration is suppressed, phonon damping is virtually negligible. Since this study is limited to very low temperatures deformation the phonon mechanism is not considered here.

For sufficiently low temperatures, the remaining mechanisms are electron damping and reradiation. Although the reradiation of elastic waves of vibrating dislocation is significant in insulators and superconductors, this mechanism is less effective than electron damping for normal metals. And the main object of this study is confined to electron damping mechanism.

As pointed out in the last section, the existence of the electron damping was first indicated in the tensile test of Pb crystal as the abnormal enhancement of plasticity due to the transition from the normal to superconducting states [2]. Creep and stress relaxation tests also confirmed the anomalies which could be ascribed to the electron damping force [8, 9, 10]. These facts are apt

to give the impression that electron damping is associated with only the normal-superconducting transition. However, effect is universal and is merely emphesized by the transition. Moreover, one should notice that it is not an easy task to extract pure component of electron damping force from the measured stress change associated with the normal-superconducting transition. For example, all the measurements were performed below the critical temperature and an external magnetic field was applied to bring the sample back to the normal state. The magnetic field might influence the dislocation behavior, either directly or indirectly through the change of electronic structure of the sample. In reality, recent experiment of Galligan [11] implies this effect. Probably only a measurement under continuous cooling through the transition temperature could resolve this point. At any rate, without overcoming these experimental difficulties, the observed difference due to the normal-superconducting transition can not be fully ascribed to the electron damping force. This point is discussed in chapter IV-4.

By the way, dislocation behavior in the superconducting state is expected to be much different from that in the normal state. Anomalous strain rate sensitivity of flow stress measured in superconducting Al and Al-Mg alloys is one of the typical examples [12],and this phenomenon is explained as the destruction of the Cooper pairs to create extra-quasi particles which is caused by dislocations moving with greater velocity than certain critical level. Various other types of quantum natures are more or less expected in the deformation properties of this state, as well. Then, as was calculated on a straight dislocation by Huffman et.al. [13] and extended to loop dislocation by Bar'yakhtar et.al. [14], it is certainly of great importance to investigate damping mechanism in superconductors utilizing a rigorous quantum mechanical treatment. However, the main scope of the present study is neither to investigate the dislocation

behavior of superconductors nor to predict new phenomenon by performing rigorous treatment. This study is confined to the electron damping mechanism in the normal state and to the discussion of possibility of the extension to many dislocations problem.

I-4. Research Problem

The previous theoretical studies of electron damping mechanism in the normal state are reviewed. The first theoretical calculation may be attributed to the classical viscosity theory of Mason [15, 16]. A dislocation is surrounded by strain field that moves with the dislocation, and free electrons in the solid exert a viscous effect on an ultrasonic wave propagated in the crystal with viscosity η. In other words a lattice vibration caused by dislocation motion can communicate energy to the free electron gas by a viscous reaction (i.e. transfer of momentum) and is damped by the viscosity of the gas. According to the classical viscosity theory of gas, the viscosity, η, is given by .

$$\eta = N m \bar{l} \frac{\bar{v}}{3} \tag{1-4}$$

where N is the number of particle, m the mass, $\bar{l}$ the mean free path, and $\bar{v}$ is the mean velocity. Mason applied the free electron gas model to the eq.1-4 and substituted the following particular quantities of free electron gas.

$$\bar{l} = \frac{\sigma m \bar{v}}{N e^2} \tag{1-5}$$

$$\overline{v^2} = \frac{3}{5} \frac{\hbar^2}{m^2} (3\pi^2 N)^{\frac{2}{3}} \tag{1-6}$$

where σ is the electrical conductivity. And as a final form, he obtained

$$\eta_e = \frac{9 \times 10^{11} \hbar^2 (3\pi^2 N)^{\frac{2}{3}}}{5 e^2 \rho} \tag{1-7}$$

where ρ is the electrical resistivity. By equating the energy dissipation associated with the viscosity η_e with the rate of change of the strain field as the dislocation moves through the crystal, the damping force and therefore the damping constant B_e was calculated for the edge dislocation

$$B_e = \frac{\frac{3}{4}b^2\eta_e}{8\pi(1-\sigma)^2 a_0^2} \tag{1-8}$$

where a_0 is the cut-off radius. Although this treatment is simple and the physics is clear, a severe inconsistency should be noticed. As was criticized by Tittmann et.al. [17], the classical viscosity theory is valid only in the case of

$$q\bar{l} \ll 1 \tag{1-9}$$

where q is the typical Fourier component of the strain field. However, the typical value of q is about the order of the reciprocal of atomic dimension and $\bar{l}$ is about 10^{-1} cm at liq. He temperature. Then $q\bar{l}$ is always far bigger than one for the electron-lattice system.

$$q\bar{l} \gg 1 \tag{1-10}$$

Therefore we should conclude that a proper electron damping can not be obtained by classical viscosity theorem.

Holstein [18] calculated the electron damping force based on perturbation method in the following way. The displacement field, $\mathbf{u}(\mathbf{r}-\mathbf{v}_D t)$, around a moving dislocation with velocity $\mathbf{v}_D$ is expanded into Fourier series.

$$\mathbf{u}(\mathbf{r}-\mathbf{v}_D t) = \sum_{\mathbf{q}} \mathbf{u}_{\mathbf{q}} \exp[i\mathbf{q}\cdot(\mathbf{r}-\mathbf{v}_D t)] + \textit{Complexconjugate} \tag{1-11}$$

Each $\mathbf{u}_{\mathbf{q}}$ is corresponding to lattice wave or lattice vibration of wave vector $\mathbf{q}$ and gives rise to a deformation potential. The total deformation potential,

$V_p(\mathbf{r})$, is, then, given as the sum of the contributions of each $\mathbf{q}$ mode.

$$V_p(\mathbf{r}) = \sum_{\mathbf{q}} i\mathbf{q}\cdot\mathbf{u}_{\mathbf{q}}\exp[i\mathbf{q}\cdot(\mathbf{r}-\mathbf{v}_D t)] + \textit{Complexconjugate} \tag{1-12}$$

Due to this deformation potential conduction electrons are scattered accompanied with the absorption or emission of phonon, $\hbar\mathbf{q}\cdot\mathbf{v}_D$ Holstein calculated the scattering probability matrix of this process by perturbation method and obtained the energy changing rate, $\frac{dW}{dt}$, in the following equation.

$$\frac{dW}{dt} = \sum_{\mathbf{k}}\sum_{\mathbf{q}}(\hbar\mathbf{q}\cdot\mathbf{v}_D)\left[f(\mathbf{k}_+)-f(\mathbf{k})\right]\frac{2\pi}{\hbar}C^2|\mathbf{q}\cdot\mathbf{u}_{\mathbf{q}}|^2\cdot\delta\left[\frac{\hbar}{m}\left(\frac{q^2}{2}+\mathbf{q}\cdot\mathbf{k}\right)-\hbar\mathbf{q}\cdot\mathbf{v}_D\right] \tag{1-13}$$

where $\hbar\mathbf{q}\cdot\mathbf{v}_D$ is the phonon energy and the remaining term expresses the transition probability of electron. $f(\mathbf{k})$ is the electron distribution function. By noticing the fact that

$$\left|\mathbf{q}\cdot\mathbf{u}_{\mathbf{q}}\right| = \left|\Delta(\mathbf{q})\right| \tag{1-14}$$

where $\Delta(\mathbf{q})$ is the Fourier transform of the dilatation, $\Delta(\mathbf{r})$, followed by several mathematical manipulations, the sum in the eq. 1-13 can be transformed into integral and the following equation is obtained.

$$\frac{dW}{dt} = \frac{L_D}{32\pi}\frac{2\pi}{\hbar}\frac{C^2}{E_F^2}\frac{q_m}{k_F}k_F^3V^2Nb^2\hbar^2\kappa \tag{1-15}$$

where L_D is the dislocation line length, q_m is the maximum q-vector corresponding to the minimum possible wave length and κ is approximately 1/4. Holstein equated this energy changing rate with power loss due to the friction force between electron and a moving dislocation of velocity v_D.

$$\frac{dW}{dt} = BL_D v_D^2 \tag{1-16}$$

A final expression of the electron damping constant, B, is obtained in the following equation.

$$B = \frac{3}{32}\frac{2\pi}{\hbar}\left(\frac{C}{E_F}\right)^2\left(\frac{q_m}{k_F}\right)k_F^3\hbar^2 N b^2 \kappa \tag{1-17}$$

On the contrary to the above perturbational approach based on quantum mechanics of Holstein, Huffman and Louat method [19, 20] described below is semi classical treatment. They calculated the electric current and electric field produced by deformation potential and moving dislocation by solving Maxwell's equation and Boltzman transport equation self-consistently. Then they obtained the friction force as a Ohm power loss which is the product of the electric current and electric field. Later, this procedure was slightly corrected by Brailsford[21] within a frame of the same physics. Their treatments are, however, straight application of the theory of ultrasonic attenuation which is traced back to the pioneer work of Cohen et.al.[22]. Essential procedures of Brailsford's are reviewed below.

The local lattice velocity, $\mathbf{u}(\mathbf{r},t)$, is expanded into the Fourier series.

$$\mathbf{u}(\mathbf{r},t) = \sum_{\mathbf{q}} \mathbf{u}_{\mathbf{q}} \exp\left[i\,\mathbf{q}\cdot(\mathbf{r}-\mathbf{v}_D t)\right] \tag{1-18}$$

where $\mathbf{v}_D$ is the dislocation velocity and Fourier coefficient $\mathbf{u}_{\mathbf{q}}$ can be considered as the phonon of wave vector $\mathbf{q}$ given by

$$\mathbf{u}_{\mathbf{q}} = \sum_{\lambda} -i\,\mathbf{q}\cdot\mathbf{v}_D \mathbf{e}_{\mathbf{q}\lambda} w_{\mathbf{q}\lambda} \tag{1-19}$$

Here λ is an index specifying the normal mode with polarization vector $\mathbf{e}_{\mathbf{q}\lambda}$, and $w_{\mathbf{q}\lambda}$ is the Fourier amplitude of the displacement associated with that mode.

Each phonon (longitudinal phonon) is associated with the dilatation field which changes the electron density. The self-consistent electric field produced by the moving dislocation change the electron density as well. This process is described by the method of distribution function $f(\mathbf{r},\mathbf{v},t)$, eq. 1-20, and Boltzman Transport Equation, 1-21[23].

$$f(\mathbf{r},\mathbf{v},t)=f^0(\mathbf{v})+f_1(\mathbf{r},\mathbf{v},t) \tag{1-20}$$

$$\frac{\partial f}{\partial t}+\mathbf{v}\frac{\partial f}{\partial \mathbf{r}}+\frac{e\mathbf{E}}{m}\frac{\partial f}{\partial \mathbf{v}}=-\frac{f-f^0}{\tau} \tag{1-21}$$

where f^0 is the equilibrium electron distribution function, f_1 is the deviation from f^0 due to the electric field $\mathbf{E}$, dilatation field and collision with impurities of which relaxation time is τ. Substitution of eq.1-20 into the eq. 1-21 followed by several mathematical manipulations yields

$$\frac{\partial f_1}{\partial t}+\mathbf{v}\nabla_{\mathbf{r}}f_1+e\mathbf{E}\mathbf{v}\frac{\partial f^0}{\partial \varepsilon}=-\frac{1}{\tau}\left[\left(m\mathbf{v}\mathbf{u}+\frac{2}{3}\frac{n_1}{n_0}\varepsilon_F\right)\frac{\partial f^0}{\partial \varepsilon}+f_1\right] \tag{1-22}$$

where n_0 is the equilibrium electron density and n_1 is the deviation from n_0 due to the dilatation field of the longitudinal phonon. The solution, f_1, of the eq. 1-22 is given by

$$f_1=-\left[\frac{\tau e\mathbf{v}\cdot\left[\mathbf{E}+\left(\frac{m\mathbf{u}}{e\tau}\right)\right]+\frac{2}{3}\varepsilon_F\left(\frac{n_1}{n_0}\right)}{1-i\omega\tau+i\mathbf{q}\mathbf{v}\tau}\right]\frac{\partial f^0}{\partial \varepsilon} \tag{1-23}$$

where ω is

$$\omega=\frac{\mathbf{q}\mathbf{b}}{\tau}-\frac{2\pi n}{\tau} \tag{1-24}$$

and n is an integer. Then, the electron current density, $\mathbf{J}$, can be calculated by

$$J = \frac{2e}{(2\pi)^3}\int f_1 v dk_x dk_y dk_z \tag{1-25}$$

and the total electric current density J_T is given by the sum of J and positive ion current density, $-en\,u$.

$$J_T = J - ne\,u \tag{1-26}$$

On the other hand, electric field E, can be correlated with J by the following Maxwell's equation.

$$div\,E = -4\pi div\,J_T \tag{1-27}$$

By solving eqs. 1-23, 1-25, 1-26 and 1-27 in a self-consistent manner, the electron current density J and electric field E can be obtained. And the product of J and E immediately gives the ohm energy loss. According to more complete calculations of Brailsford, the energy absorption rate P_q of a longitudinal phonon of q is approximated to

$$P_q = \frac{\hbar n_0 m}{\tau}\left[1+\left(\frac{q}{q_{TF}}\right)^2\right]^{-2}\frac{1}{8}\pi q l_e^{-}\left|u_{q\parallel}\right|^2 \tag{1-28}$$

where q_{TF} is the reciprocal of Thomas-Fermi screening length. Since the transversal phonon contribution is found to be negligibly small the total energy loss rate, dW/dt, is given by the sum of P_q

$$\frac{dW}{dt} = \sum_q P_q \tag{1-29}$$

The final step to obtain the damping constant B_e is quite the same with that of Holstein's procedure, eq. 1-16. And the final expression for B_e is given by

$$B_e = \left(\frac{1-2\nu_p}{1-\nu_p}\right)^2 \frac{n_0 m v_F b^2 q_d}{96}\Phi\left(\frac{q_D}{q_{TF}}\right) \tag{1-30}$$

where

$$\Phi(x)=\frac{1}{2}[(1+x^2)^{-1}+x^{-1}\tan^{-1}x] \tag{1-31}$$

and q_D is the radius of Debye sphere.

Both the perturbational approach of Holstein and the self-consistent Boltzman Transport Equation method of Brailsford are very elegant method, however, the following two points are open to question.

In general, by introducing a N+1 dimensional coordinate system which consists of N coordinate for atomic displacements of each N atoms and the other coordinate for a potential energy of the system, the dislocation motion in a crystal of N atoms can be characterized as a trace along a one dimensionally extended saddle points configuration in the space. And the displacement of each atom caused by the motion of a dislocation can be given by the sum of a displacement corresponding to the saddle points and the deviation. The first component (saddle points) is so-called dislocation coordinate and the latter one (deviation) is regarded as phonon. Although, both Holstein and Brailsford treated a moving dislocation essentially as a wave packet of phonon, as discussed by Ninomiya [60], the dislocation coordinate given within an approximation of linear continuum elasticity theory does not always coincide with the saddle points but deviates. Then, in order to treat a dislocation motion as a phonon, one should be careful about not only allowable limit of the wavelength of phonon but also the width of the dislocation core which gives a measure of the applicability of continuum approximation.

Secondly, the right-hand side of eq. 1-21 is a scattering term but the mechanism is not specified clearly. If it is caused by impurities as was assumed by Cohen et.al. [22], the final result must be modified by the concentration term.

The theoretical calculation carried out in this study may not provide self-consistent solution but demonstrates different approach to the electron damping problem.

This study proceeds in the following order. In chapter II, general formulation based on the special theory of relativity is carried out. Beginning with a brief review of Lorentz transformation, two essential coordinate systems are introduced to characterize the dislocation motion, and finally Maxwell's equations appropriate to this problem is established. The chapter III is devoted to the calculation procedures. In the first section, calculations of electrostatic potential and electron density are performed by introducing Cottrell et.al's traditional work. The second section is the heart of this calculation and mathematically elegant Mackenzie and Sondheimer's procedures are introduced to set up and to solve Boltzman Transport Equation. The final product is expressed as the electrical resistivity. The third section is the calculation of the friction force using the electric resistivity obtained in the former section. And in the last section, numerical calculations of magnetic induction are introduced. In the chapter IV, the results obtained in the chapter III are discussed. The first three sections discuss the applicability of the Born approximation and the intrinsic inconsistency of Mackenzie-Sondheimer's method. The fourth section is the main discussion of the friction force. The method of the experimental analysis is examined, and in order to compare the calculated results more reliably, electric resistivity data are also introduced. The discrepancy is discussed by referring to Matthiesen's rule. In the fifth section, the calculated magnetic induction value is shown to be negligible. The last section is unclosed work. The possibility of the extension of present study to many body problem (collective behavior of dislocations) is discussed.

II. ELECTRODYNAMICAL FORMULATION OF AN EDGE DISLOCATION MOTION

II-1. Maxwell's Equations and Lorentz Transformation

Although dislocation velocities have never been observed to exceed ~10^3 cm/sec and any relativistic effects are hardly expected, the basic idea posed in the model, namely motion of charged particles associated with moving dislocation, essentially belongs to electrodynamics. Therefore it is of basic interest to formulate this problem in a strict manner based on the special theory of relativity of Einstein.

The tensor expression of Maxwell's Equations in Lorentz gauge are given by the following sets of equations [24].

$$F_{\mu\nu} = \frac{\partial A_\nu}{\partial x_\mu} - \frac{\partial A_\mu}{\partial x_\nu} \tag{2-1}$$

$$\Box A_\mu = -\frac{1}{c\,\varepsilon_0} j_\mu \tag{2-2}$$

and

$$\frac{\partial A_\mu}{\partial x_\mu} = 0 \tag{2-3}$$

where $\Box$ is the Lorentz invariant four dimensional Laplacian more explicitly expressed as

$$\Box = \nabla^2 - \frac{1}{c^2}\frac{\partial^2}{\partial t^2} \tag{2-4}$$

A_μ, $F_{\mu\nu}$ and j_μ are the 4-vector potential, field-strength tensor, and charge-current 4-vector, respectively, and are concise notation of the following matrix.

$$(A_\mu) = (c\,\mathbf{A}, i\varphi) \tag{2-5}$$

$$(F_{\mu\nu}) = \begin{bmatrix} 0 & cB_z & -cB_y & -iE_x \\ -cB_z & 0 & cB_x & -iE_y \\ cB_y & -cB_x & 0 & -iE_z \\ iE_x & iE_y & iE_z & 0 \end{bmatrix} \tag{2-6}$$

$$(j_\mu) = \begin{pmatrix} i_x \\ i_y \\ i_z \\ ic\rho \end{pmatrix} \tag{2-7}$$

where c is the velocity of light, $\mathbf{A}$ is the vector potential, φ, is the scalar potential, $\mathbf{E}(E_x, E_y, E_z)$ is the electronic field, $\mathbf{B}(B_x, B_y, B_z)$ is the magnetic flux density, $\mathbf{i}(i_x, i_y, i_z)$ is the current density and ρ is the charge density.

The Lorentz transformation is characterized as an invariant transformation which conserves the distance between two points in 4-dimensional Minkowski Space. The transformation law between the coordinates x_ν and $x'_\mu(\nu,\mu;1,2,3,4)$ in two inertia systems, K and K', are given by

$$x'_\mu = a_{\mu\nu} x_\nu \tag{2-8}$$

x_μ consists of three dimensional space coordinates, x, y, z and one dimensional time coordinate, t.

$$\begin{pmatrix} x_1 \\ x_2 \\ x_3 \\ x_4 \end{pmatrix} = \begin{pmatrix} x \\ y \\ z \\ ict \end{pmatrix} \tag{2-9}$$

In the special case where system K' has its coordinate axes parallel to those of K and is moving with a constant relative velocity v in the x direction, the transformation matrix $a_{\mu\nu}$ in the eq. 2-8 can be simplified and is given by the following matrix.

$$(\alpha_{\mu\nu}) = \begin{bmatrix} \frac{1}{\sqrt{1-\beta^{*2}}} & 0 & 0 & \frac{i\beta^*}{\sqrt{1-\beta^{*2}}} \\ 0 & 1 & 0 & 0 \\ 0 & 0 & 1 & 0 \\ \frac{-i\beta^*}{\sqrt{1-\beta^{*2}}} & 0 & 0 & \frac{1}{\sqrt{1-\beta^{*2}}} \end{bmatrix} \tag{2-10}$$

where

$$\beta^* = \frac{v}{c} \tag{2-11}$$

Covariance of the Maxwell's equations with respect to Lorentz transformation between two inertia system is an important consequence of the theory of relativity, and 4-vector potentials, A_ν and A'_μ, defined in the two systems are related by the following transformation law with the same transformation matrix 2-10.

$$A'_\mu = \alpha_{\mu\nu} A_\nu \tag{2-12}$$

II-2. Representation of a Moving Edge Dislocation in Two Inertia Coordinate Systems

Physical phenomena associated with a dislocation moving in a positive x direction with constant velocity v can be described in various coordinate systems. Among them, the following two orthogonal coordinate systems, K and K', are of specific interest in this study.

In the K-system, the coordinate is fixed to the lattice and the dislocation moves, in the positive x direction with a constant velocity, v, with respect to this lattice. On the other hand, in the K'-system whose origin is fixed on the core of the dislocation, the coordinate moves with the dislocation. Therefore, in the K'-system, media surrounding the dislocation moves in the negative x' direction with velocity v. The configurational relation among the K-system, K'-system and the dislocation is shown in Fig. 1.

Due to the introduction of an edge dislocation, a displacement field is induced. In the K-system, components of the displacement field, u_x^K, u_y^K, u_z^K in the x,y,z direction, respectively, are given by [25]

$$u_x^K = \frac{b}{2\pi}\left[\frac{2v_s^2}{v^2}\right]\left\{\tan^{-1}\frac{\gamma y}{x-vt} - \alpha^2\tan^{-1}\frac{\beta y}{x-vt}\right\} \tag{2-13}$$

$$u_y^K = \frac{b}{2\pi}\left[\frac{2v_s^2}{v^2}\right]\left\{\gamma\ln\{(x-vt)^2+(\gamma y)^2\}^{\frac{1}{2}} - \left[\frac{\alpha^2}{\beta}\right]\ln\{(x-vt)^2+(\beta y)^2\}^{\frac{1}{2}}\right\} \tag{2-14}$$

and

$$u_z^K = 0 \tag{2-15}$$

where superscript K stands for the K-system, v_s is the transverse velocity of sound, and α,β,γ are given by the following relations with longitudinal sound velocity v_l.

$$\alpha = \left\{1-\left[\frac{v^2}{2v_s^2}\right]\right\}^{\frac{1}{2}} \tag{2-16}$$

$$\beta = \left\{1-\left[\frac{v^2}{v_s^2}\right]\right\}^{\frac{1}{2}} \tag{2-17}$$

$$\gamma = \left\{1-\left[\frac{v^2}{v_l^2}\right]\right\}^{\frac{1}{2}} \tag{2-18}$$

and superscript K stands for the K-system.

In the K'-system, however, these components are modified according to the Lorentz transformation in the following way.

$$u_x^K = \frac{b}{2\pi}\left[\frac{2v_s^2}{v^2}\right]\left\{\tan^{-1}\frac{\gamma y'}{\delta x'} - \alpha^2\tan^{-1}\frac{\beta y'}{\delta x'}\right\} \tag{2-19}$$

$$u_y^{K'} = \frac{b}{2\pi}\left[\frac{2v_s^2}{v^2}\right]\left[\gamma\ln\{(\delta x')^2+(\gamma y')^2\}^{\frac{1}{2}} - \frac{\alpha^2}{\beta}\ln\{(\delta x')^2+(\beta y')^2\}^{\frac{1}{2}}\right] \tag{2-20}$$

and

$$u_z^{K'} = 0 \tag{2-21}$$

where

$$\delta = \sqrt{1-(\beta^*)^2} \tag{2-22}$$

and the next relations derived from eqs. 2-8 and 2-10 were employed.

$$\begin{bmatrix} x \\ y \\ z \\ ict \end{bmatrix} = \begin{bmatrix} \frac{1}{\delta}(x'+vt') \\ y' \\ z' \\ \frac{i}{\delta}(\beta^* x'+ct') \end{bmatrix} \tag{2-23}$$

The dilatation field, $\Delta_{K'}$, is calculated from the components of the displacement field obtained above.

$$\Delta_{K'} = \frac{\partial u_i^{K'}}{\partial x_i'}$$

$$= \frac{b}{2\pi}\left[\frac{2v_s^2}{v^2}\right]\left\{\frac{\gamma y'(\gamma^2-\delta)}{(\delta x')^2+(\gamma y')^2} + \frac{\alpha^2\beta(\delta-1)y'}{(\delta x')^2+\beta y'^2}\right\} \tag{2-24}$$

where $(x_1', x_2', x_3')=(x', y', z')$, and $(u_1', u_2', u_3')=(u_x', u_y', u_z')$. Because of this dilatation field the positive charge density (positive ionic density), ρ_K^+ becomes heterogeneous and is given by

$$\rho_K^+ = \rho_{0K}^+(1+\Delta_K)^{-1}$$

$$= \frac{\rho_{0K}^+}{\delta}(1+\Delta_K)^{-1} \tag{2-25}$$

where ρ^{+}_{oK} and $\rho^{+}_{oK'}$ are uniform positive charge densities of the dislocation free crystal represented in K- and K'-system, respectively, and the modification from the first equation to the second one is a direct consequence of the Lorentz contraction. It should be noticed that the explicit time term can be neglected in the K'-system representation eq. 2-24, while not in the K-system formulation.

II-3 Establishment of Maxwell's Equations for a Moving Edge Dislocation

Further discussions are developed in the K'-system instead of K-system, because, as was recognized in the last section, the explicit time term disappears in the dilatation, eq. 2-24, and therefore the K'-system is easier to handle mathematically. If need be, the covariant property of Maxwell's equations, eq. 2-12, allow the solution to be easily transformed into that of K-system. Main interest is confined to the steady state, therefore the 4-dimensional Laplacian, $\Box$ can be simplified to the 3-dimensional Laplacian, ∇^2, and Maxwell's equation can be rewritten as

$$\nabla^2(') A'_\mu = -\frac{1}{c\,\varepsilon_0} j'_\mu \tag{2-26}$$

Here, by making use of the results obtained in the last section, components of the charge-current 4-vector j'_μ are given by

$$(j'_\mu) = \begin{Bmatrix} -\dfrac{\rho^{+}_{oK}}{\delta} v \\ 0 \\ 0 \\ ic\{\rho_{\vec{K}} - \rho^{+}_{oK}(1+\Delta_K)^{-1}\} \end{Bmatrix} \tag{2-27}$$

where $\rho_{\vec{K}}$ is the unknown electron density which plays an essential role in this study. Substitution of eqs. 2-5 and eq. 2-27 into eq. 2-26 establishes more explicit form of Maxwell's equations in the following way.

$$\nabla^2(')A_z = \frac{1}{c^2\varepsilon_0}\left[\frac{\rho_{0K}^{+}}{\delta}v\right] \tag{2-28}$$

$$\nabla^2(')A_y = 0 \tag{2-29}$$

$$\nabla^2(')A_x = 0 \tag{2-30}$$

$$\nabla^2(')\varphi = -\frac{1}{\varepsilon_0}\{\rho_K^{-} - \rho_{0K}^{+}(1+\Delta_K)^{-1}\} \tag{2-31}$$

III. CALCULATION PROCEDURES

III-1. Electrostatic Potential and Electron Density Around a Dislocation

A rigorous treatment based on special theory of relativity was demonstrated in the last chapter. But as pointed out previously, dislocation velocities are less than $\sim 10^3$ cm/sec which is negligible as compared to the speed of light. Therefore, β^* in the eq.2-11 and δ in the eq.2-22 can be put to 0 and 1, respectively. This operation mathematically corresponds to the reduction of the Lorentz transformation, eq. 2-23, to the following Galilei transformation

$$\begin{pmatrix} x \\ y \\ z \\ t \end{pmatrix} = \begin{pmatrix} x'+vt' \\ y' \\ z' \\ t' \end{pmatrix} \tag{3-1}$$

and physically means that every phenomena is observed at the same time in both K- and K'- system. In particular, this study of dislocation motion can be reduced to a treatment within a frame of electrostatics, and the first task is to obtain the electrostatic potential and electron density around a moving edge dislocation by focusing on the last equation 2-31 of Maxwell's equation.

The dilatation field around a dislocation causes the Fermi energy to change from place to place. Physical origins of this change are two-fold; change of the kinetic energy of electrons due to the change of wave length and change of ground level energy, both caused by lattice dilatation. However, in the equilibrium state the electrochemical potential should be a constant through the whole crystal, therefore electron redistribution takes place so that the electrostatic potential produced by the redistributed electrons compensates the Fermi energy change. This mechanism was originally developed by Cottrell et.al.[26] in order to estimate the electric interaction energy between a

static edge dislocation and a solute atom of different valence.

Mathematically, these mechanisms are described in the following equations. The Fermi energy around an edge dislocation is given by

$$\varepsilon_F(r) = \varepsilon_G' + \frac{\hbar^2}{2m} k_F'^2$$

$$\cong \varepsilon_G^0 + \varepsilon_1 \Delta + \frac{\hbar^2}{2m} k_F^2 (1+\Delta)^{-\frac{2}{3}} \qquad (3\text{-}2)$$

where ε_G^0 and ε_G' are ground level energies of perfect and distorted crystals, k_F and k_F' are the Fermi vectors of those crystals, respectively. In the above equations a Taylor expansion with respect to dilatation, Δ, is carried out on ground level energy, ε_G', and the first two terms are considered. ε_1 could be found by the following fact; the equilibrium lattice parameter is determined by the condition that the derivative of the total energy of the conduction electrons with respect to Δ should vanish at $\Delta=0$. Thus,

$$\varepsilon_1 = \frac{2}{5} \frac{\hbar^2 k_F^2}{2m} \qquad (3\text{-}3)$$

On the other hand, the condition of constant electrochemical potential is given by

$$\mu(r) = \varepsilon_F^0$$

$$= \varepsilon_F(r) - e\varphi(r) \qquad (3\text{-}4)$$

where $\mu(r)$ is the electrochemical potential at $r(x',y',z')$ which is equivalent to the Fermi energy of a perfect crystal (or Fermi energy at the region infinitely far away from a dislocation) and $\varphi(r)$ is the electrostatic potential after the electron redistribution. Although, from eq.3-2, the change of the Fermi energy,

$\delta\varepsilon_F(\mathbf{r})$, can be given by

$$\delta\varepsilon_F(\mathbf{r}) = \varepsilon_F(\mathbf{r}) - \varepsilon_F^0$$

$$= -\frac{4}{15}\frac{\hbar^2}{2m}k_F^2\Delta(r) \tag{3-5}$$

and this net amount was implied to be compensated by electron redistribution in the Cottrell's treatment, because of the electric field produced by positive ions. $\delta\varepsilon_F(\mathbf{r})$ can not be directly equated to $e\varphi(\mathbf{r})$ in eq. 3-4. Proper solution should be obtained by the simultaneous and self-consistent solutions of equations 2-31 and 3-4.

In order to proceed to actual computations the Thomas-Fermi approximation is performed on $\varepsilon_F(\mathbf{r})$ and eq. 3-4 is rewritten in terms of electron density, $\rho_K^-(\mathbf{r})$, in the next equation

$$\rho_K^-(\mathbf{r}) = \rho_{0K}^-\left[1-\frac{2}{5}\Delta+\frac{e\varphi}{\varepsilon_{kin}^0}\right]^{\frac{3}{2}} \tag{3-6}$$

where ε_{kin}^0 is the kinetic energy of electron in a perfect crystal and is given by

$$\varepsilon_{kin}^0 = \frac{\hbar^2 k_F^2}{2m} \tag{3-7}$$

Here, the simultaneous equations which give the equilibrium electron density and electrostatic potential around an edge dislocation are set up in the following way

$$\rho^- = \rho_0^-\left[1-\frac{3}{5}\Delta+\frac{3}{2}\frac{e\varphi}{\varepsilon_{kin}^0}\right] \quad (\textit{provided that } -\frac{2}{5}\Delta+\frac{e\varphi}{\varepsilon_{kin}^0} \ll 1) \tag{3-8}$$

$$\nabla^2\varphi = -\frac{1}{\varepsilon_0}\{\rho^- - \rho_0^-(1+\Delta)^{-1}\} \tag{3-9}$$

and

$$\rho_0^+ = \rho_0^- = \rho_0 \tag{3-10}$$

where the subscript K' is neglected in order to avoid unnecessary complications.

Since it is quite tedious to demonstrate whole calculations of these simultaneous equations essential steps of the procedures are briefly summarized below.

Substitution of eq. 3-8 into eq. 3-9 yields the following partial differential equation (P.D.E) in a infinite two dimensional space.

$$(\nabla^2 - \alpha)\varphi(\mathbf{r}) = D\Delta(\mathbf{r}) \tag{3-11}$$

$$\varphi \in R_2 \text{ and } \varphi \to 0 \text{ at } |\mathbf{r}| \to \infty$$

where α and D are given by

$$\alpha = \frac{6\pi e^2 \rho_0}{\varepsilon_{Con}^0} \tag{3-12}$$

and

$$D = \frac{8}{5}\pi e \rho_0 \tag{3-13}$$

respectively, and instead of the notation of Laplacian operator Δ, "$\nu\alpha\beta\lambda\alpha$" operator, ∇^2, is used. The corresponding fundamental equation of P.D.E. 3-11 is given by

$$(\nabla^2 - \alpha)g_2(\mathbf{r}|\xi) = -\delta(\mathbf{r}-\xi) \tag{3-14}$$

and the Green's function is explicitly given by [27]

$$g_2(\mathbf{r}|\xi) = \frac{1}{2\pi}K_0(\sqrt{\alpha}\,|\mathbf{r}-\xi|) \tag{3-15}$$

where K_0 is the 0-th order modified Bessel function of the 2nd kind. Therefore, with the aid of the Green's function the solution of P.D.E., 3-11 is obtained as

$$\varphi(\mathbf{r}) = -\int\int_{R_\xi} g_2(\mathbf{r}|\xi)D\Delta(\xi)d\xi$$

$$= -\frac{D}{\alpha}(\Delta(\mathbf{r})-2C\sqrt{\alpha}K_1(\sqrt{\alpha}\,|\mathbf{r}|)\frac{\sin\vartheta}{\gamma+1}+\int\int_{R_\xi} g_2(\mathbf{r}|\xi)\nabla^2\Delta d\xi) \tag{3-16}$$

$$C=\left(-\frac{\delta}{2}\pi\right)2\left(\frac{v_s}{v_l}\right)^2 \tag{3-17}$$

where K_1 is the 1st order modified Bessel function of the 2nd kind, γ was given in the eq. 2-18 and ϑ is measured anticlockwise from positive x' axis. In the eq. 3-16, the reduction of the upper integral into the lower equation is quite hard and despite of the persistent attacks with various mathematical techniques $\varphi(\mathbf{r})$ could not be fully expressed by well defined functions. In order to evaluate the contribution of the 3rd term the integration was numerically performed for various physically meaningful values of α and γ, and the results were compared with 1st and 2nd term. Several results are shown in Figs. 2, 3 and 4. One can see that the 3rd term is negligibly small and can be safely neglected in the eq. 3-16. Therefore the final form of electrostatic potential $\varphi(\mathbf{r})$ is well approximated to

$$\varphi(\mathbf{r})=-\frac{D}{\alpha}\left(\Delta(\mathbf{r})-2\sqrt{\alpha}CK_1(\sqrt{\alpha}\,|\mathbf{r}|)\frac{\sin\vartheta}{\gamma+1}\right) \tag{3-18}$$

and substitution of the eq. 3-18 into eq. 3-8 yields

$$\rho^-(\mathbf{r}) = \rho_0\left(1-\Delta+\frac{4}{5}C\sqrt{\alpha}K_1(\sqrt{\alpha}\,|\mathbf{r}|)\frac{\sin\vartheta}{\gamma+1}\right) \tag{3-19}$$

These numerical processes are discussed in the section IV-1 again but it is noticeable that in the case of a static dislocation the 3rd term in the eq. 3-16 automatically vanishes and $\varphi(\mathbf{r})$ is strictly expressed as

$$\varphi(\mathbf{r}) = -\frac{4}{15}\frac{1}{e}\frac{\hbar^2 k_F^2}{2m}(\Delta(r) - C\sqrt{a}\,K_1(\sqrt{a}\,|\mathbf{r}|)\sin\vartheta) \tag{3-20}$$

which includes extra screening contribution, the 2nd term, as compared with $\delta\varepsilon_F(\mathbf{r})$ of the eq. 3-5.

III-2. Establishment of Boltzman Transport Equation and Mackenzie-Sondheimer's Procedures

Various transport phenomena in a crystal can be well described by means of Boltzman Transport Equation (B.T.E.). Since the general features of this equation are discussed in detail in many articles, The essential points of this equation are briefly reviewed in this section and the B.T.E appropriate for this particular dislocation problem is established. In order to obtain the electrical resistivity by solving the B.T.E. analytically, classical Mackenzie-Sondheimer's procedures are introduced.

III-2-1. Establishment of Boltzman Transport Equation

Let $f(\mathbf{k},\mathbf{r},t)$ be the electron distribution function in a phase space. Under the given circumstances which are specified in the B.T.E., the probability of finding the electron of state $\mathbf{k}$ (momentum), at time t, in the space $\mathbf{r}$, is described by this function. And this function as the solution of the B.T.E. plays the essential role in the study of transport phenomena. In the steady state the distribution function should satisfy the following condition.

$$\frac{df}{dt} = \left.\frac{\partial f}{\partial t}\right|_{drift} + \left.\frac{\partial f}{\partial t}\right|_{field} + \left.\frac{\partial f}{\partial t}\right|_{scattering} = 0 \tag{3-21}$$

The drift and field terms are more explicitly given by

$$\left.\frac{\partial f}{\partial t}\right|_{drift} = -\mathbf{v}_{\mathbf{k}}\cdot\nabla_{\mathbf{r}} f \tag{3-22}$$

and

$$\left.\frac{\partial f}{\partial t}\right|_{field} = -\frac{e}{\hbar}\left[\mathbf{E}+\frac{1}{c}\mathbf{v}_{\mathbf{k}}\times\mathbf{H}\right]\cdot\nabla_{\mathbf{k}} f \tag{3-23}$$

where $\nabla_{\mathbf{r}}$ and $\nabla_{\mathbf{k}}$ are the vector differential operators in a phase space with respect to space coordinate $\mathbf{r}$ and momentum coordinate $\mathbf{k}$, respectively; $\mathbf{v}_{\mathbf{k}}$ is the group velocity of electron; $\mathbf{E}$ is the external electric field and $\mathbf{H}$ is the external magnetic field. The scattering term is discussed later in detail. In the equilibrium state, the distribution function is the familiar Fermi-Dirac distribution function, $f^0(\mathbf{k})$, given by

$$f^0(\mathbf{k}) = \frac{1}{\exp[(\varepsilon(\mathbf{k})-\zeta)/kT]+1} \tag{3-24}$$

where ε is the energy of electron and ζ is the electrochemical potential. By following Ziman [23], the steady state distribution function, $f(\mathbf{k},\mathbf{r})$, is assumed not to depart very far from equilibrium distribution function, f^0, and the function $G(\mathbf{k},\mathbf{r})$ is assigned to describe this small deviation.

$$G(\mathbf{k},\mathbf{r}) = f(\mathbf{k},\mathbf{r})-f^0(\mathbf{k}) \tag{3-25}$$

Substitution of eqs. 3-22~3-25 into the eq. 3-21 yields

$$\left[-\frac{\partial f^0}{\partial \varepsilon}\right]\mathbf{v}_{\mathbf{k}}\left[-\frac{(\varepsilon(\mathbf{k})-\zeta)}{T}\nabla_{\mathbf{r}}T+e\left[\mathbf{E}-\frac{1}{e}\nabla_{\mathbf{r}}\zeta\right]\right]$$

$$= -\left.\frac{\partial f}{\partial t}\right|_{scattering} +\mathbf{v}_{\mathbf{k}}\cdot\nabla_{\mathbf{r}}G+\frac{e}{\hbar}(\mathbf{v}_{\mathbf{k}}\times\mathbf{H})\cdot\nabla_{\mathbf{k}}G \tag{3-26}$$

Interest here, however, is restricted to the case of homogeneous spatial temperature distribution, T, with the absence of magnetic field, H, therefore, above eq. 3-26 is greatly simplified to

$$\left(-\frac{\partial f^0}{\partial \varepsilon}\right)\nabla_{\mathbf{k}}\{e(\mathbf{E}-\frac{1}{e}\nabla_{\mathbf{r}}\zeta)\} = -\left.\frac{\partial f}{\partial t}\right|_{scattering} \tag{3-27}$$

Moreover, as was demonstrated in the last section, the spatial heterogeneity of electrochemical potential due to the introduction of a dislocation is canceled out by electron redistribution; therefore, eq.3-27 can be simplified further.

$$\left(-\frac{\partial f^0}{\partial \varepsilon}\right)\nabla_{\mathbf{k}} e\,\mathbf{E} = -\left.\frac{\partial f}{\partial t}\right|_{scattering} \tag{3-28}$$

Here the scattering term in the eq.3-21 is discussed. In this study, two scattering mechanisms are assumed. One is thermal sattering and the other is dislocation scattering which is the particular feature of this model.

$$\left.\frac{\partial f}{\partial t}\right|_{scattering} = \left.\frac{\partial f}{\partial t}\right|_{therm.} + \left.\frac{\partial f}{\partial t}\right|_{disloc.} \tag{3-29}$$

The actual mechanism of the thermal scattering is complicated, but without going into the detail this effect can be expressed by

$$\left.\frac{\partial f}{\partial t}\right|_{therm.} = -\frac{f(\mathbf{k})-f^0}{\tau} \tag{3-30}$$

where τ is the relaxation time and all the complicated physical mechanisms of thermal scattering are enclosed into this "parameter". On the other hand, the mechanism of dislocation scattering is well described in the following equation.

$$\left.\frac{\partial f}{\partial t}\right|_{disloc.} = C_0\{\int\int_{\mathbf{k}'}\int f(\mathbf{k}')(1-f(\mathbf{k}))Q(\mathbf{k}',\mathbf{k})d\mathbf{k}' - \int\int_{\mathbf{k}'}\int f(\mathbf{k})(1-f(\mathbf{k}'))Q(\mathbf{k},\mathbf{k}')d\mathbf{k}'\}$$

(3-31)

where C_0 is a constant and $Q(\mathbf{k}',\mathbf{k})$ is the transition probability from $\mathbf{k}'$-state to $\mathbf{k}$-state per unit time. Therefore, the first integral describes the incoming rate to $\mathbf{k}$-state from all other states, the second integral describes the outgoing rate from $\mathbf{k}$-state to other states and hence the whole right hand side means the net change of $\mathbf{k}$-state. Since scattering causes merely the change of state, only $\mathbf{k}$ or $\mathbf{k}'$ is explicitly written in the arguments of distribution function f. The physical mechanism of the dislocation scattering is directly reflected in the transition probability, $Q(\mathbf{k},\mathbf{k}')$, which is given by (APPENDIX A)

$$Q(\mathbf{k},\mathbf{k}') = \frac{\pi}{\hbar^2}|\langle \mathbf{k}'|\Delta U|\mathbf{k}\rangle|^2\delta\left(\frac{\Delta\varepsilon}{2\hbar}\right) \tag{3-32}$$

where Dirac's bra-ket notation is used for the matrix element and $|\mathbf{k}\rangle$ describes the free electron wave function. (ket is the complex conjugate.)

$$|\mathbf{k}\rangle \sim e^{i\mathbf{k}\cdot\mathbf{r}} \tag{3-33}$$

The argument of the delta function appearing in the eq. 3-32 is the simple difference in energy between $\mathbf{k}$ and $\mathbf{k}'$ states and is given by

$$\Delta\varepsilon = \varepsilon(\mathbf{k}) - \varepsilon(\mathbf{k}') \tag{3-34}$$

Then any inelastic scattering processes are neglected in this study. As shown in APPENDIX A, this transition probability is derived within a frame of Born approximation [28] as the elastic free electron scattering process due to the presence of perturbation (scattering) field, ΔU. As the perturbation potential, ΔU, of an edge dislocation, the electrostatic potential field derived in the last section is employed.

$$\Delta U(\mathbf{r}) = -e\,\varphi(\mathbf{r}) \tag{3-35}$$

And the substitution of eqs. 3-29~3-32 and 3-35 into the eq. 3-28 immediately yields the B.T.E. for this study in the following form.

$$\left(-\frac{\partial f^0}{\partial \varepsilon}\right)\mathbf{v}_{\mathbf{k}}\cdot e\mathbf{E} = \frac{f(\mathbf{k})-f^0}{\tau} - C_0\frac{\pi}{\hbar^2}\int_{\mathbf{k}'}\int\left(f(\mathbf{k}')-f(\mathbf{k})\right)|\langle\mathbf{k}'|-e\varphi|\mathbf{k}\rangle|^2\delta\left(\frac{\Delta\varepsilon}{2\hbar}\right)d\mathbf{k}' \tag{3-36}$$

where the reduction of the integrands in the eq.3-31 to the eq.3-36 is based on the principle of microscopic reversibility [29]. The construction of the B.T.E. is, in principle, completed by the above equation 3-36 and the remaining task is to solve this integral equation. Although the appearance of the eq. 3-36 is complicated, mathematical techniques make it possible to reduce the triple integral to a single integral. The details of the whole procedure are quite tedious, and only the essential points are described here.

The key role is played by δ-functions in the integrand. The first reduction from triple integral to double integral is rather a conventional technique often used in solid state physics [30]. The volume element in the $\mathbf{k}'$-space, $d\mathbf{k}'$, is split into the product of two terms $dS_{\mathbf{k}}$ and $dK'_{\perp}$.

$$d\mathbf{k}' = dS_{\mathbf{k}}\cdot dK'_{\perp} \tag{3-37}$$

where $dS_{\mathbf{k}}$ is the surface element of the equi-energy surface in the $\mathbf{k}'$-space and $dK'_{\perp}$ is the normal element to this surface, which satisfies the following condition

$$dK'_{\perp} = \frac{d\varepsilon(\mathbf{k}')}{|\nabla_{\mathbf{k}'}\varepsilon(\mathbf{k}')|}$$

$$= \frac{d\varepsilon(\mathbf{k}')}{|\hbar\mathbf{v}_{\mathbf{k}'}|} \tag{3-38}$$

here, from the first line to the second line, the definition of the group velocity,

$\mathbf{v}_{\mathbf{k}}$, of electron is applied. By substituting the eqs. 3-37 and 3-38 into the eq. 3-36 followed by the operation of the δ-function, $\delta(\frac{\Delta\varepsilon}{2\hbar})$, the volume integral is reduced to a surface integral over the equi-energy surface $S_{\varepsilon(\mathbf{k})}$.

$$\int\int_{\mathbf{k}}\int (f(\mathbf{k}')-f(\mathbf{k}))|\langle\mathbf{k}'|-e\varphi|\mathbf{k}\rangle|^2\cdot\delta\left(\frac{\Delta\varepsilon}{2\hbar}\right)d\mathbf{k}'$$

$$= \frac{2m}{\hbar k}\int\int_{equienergysurface}(f(\mathbf{k}')-f(\mathbf{k}))|\langle\mathbf{k}'|-e\varphi|\mathbf{k}\rangle|^2 dS_{\mathbf{k}'} \qquad (3\text{-}39)$$

The coefficient term of the right hand side originates from both the denominator of the eq. 3-38 and the argument in the δ-function, but is written in terms of $\mathbf{k}$-vector instead of velocity, $\mathbf{v}$, which are related to each other by the momentum equation of the free electron.

$$m\mathbf{v} = \hbar\mathbf{k} \qquad (3\text{-}40)$$

The second reduction, from double integral to single integral, requires more tedious variable transformations, but the essential point is again ascribed to the delta function as is mentioned below. One will notice that the scattering probability matrix, $S_{\mathbf{kk}'}$, which is given by

$$S_{\mathbf{kk}'} = \langle\mathbf{k}'|\Delta U|\mathbf{k}\rangle \qquad (3\text{-}41)$$

is mathematically equivalent to the Fourier transformation of the perturbation potential field in a real space into the 3-dimensional K-space. However, ΔU is essentially two dimensional function of x and y, because the dilatation $\Delta(\mathbf{r})$, given by eq. 2-24, which constitutes ΔU is constant in the z-direction. Then the delta function comes out in the K_z-direction.

$$S_{\mathbf{kk}'} = \langle\mathbf{k}'|\Delta U(x,y,z)|\mathbf{k}\rangle$$

$$= 2\pi\delta(K_z)\langle \mathbf{k}'|\Delta U(x,y)|\mathbf{k}\rangle_2 \tag{3-42}$$

where subscript 2 indicates the dimension and K_z is the z-component of the vector $\mathbf{K}$ defined by

$$\mathbf{K} = \mathbf{k}'-\mathbf{k} \tag{3-43}$$

Observing that the equi-energy surface for free electron is sphere surface, the Polar coordinate system is introduced (Fig. 5).

$$k_x = k\cdot\sin\vartheta\cdot\cos\varphi \tag{3-44}$$

$$k_y = k\cdot\sin\vartheta\cdot\sin\varphi \tag{3-45}$$

$$k_z = k\cdot\cos\vartheta \tag{3-46}$$

The surface integral appearing in the eq. 3-39 is, therefore, transformed to double integral with respect to ϑ' and φ' for constant k-value. And the δ-function singled out in the eq. 3-42 immediately reduces it to single integral along the φ' for constant ϑ value, ie. $\vartheta'=\vartheta$, because

$$K_z = k_z'-k_z$$

$$= k(\cos\vartheta'-\cos\vartheta) \tag{3-47}$$

Now the final form of the B.T.E. can be given by

$$(-\frac{\partial f^0}{\partial \varepsilon})e\,\mathbf{v}_k\cdot\mathbf{E} = \frac{f(\mathbf{k})-f^0}{\tau} - C'\int_{\varphi'}(f(\mathbf{k}')-f(\mathbf{k}))|\langle \mathbf{k}'|-e\varphi|\mathbf{k}\rangle_2|^2 d\varphi' \tag{3-48}$$

where C' represents material and physical constant.

As is shown in the original work of Mackenzie and Sondheimer [56], the solution of this integral equation can be found by successive approximation

method (Neumann Series) [31] after the following variable transformation.

$$G(\mathbf{k},\mathbf{r}) = f(\mathbf{k},\mathbf{r}) - f^0(\mathbf{k}) \tag{3-25}$$

$$= -\frac{\hbar}{m}\mathbf{g}(\mathbf{k})\cdot\mathbf{k}\frac{\partial f^0}{\partial \varepsilon} \tag{3-49}$$

and

$$-e\,\mathbf{k}\cdot\mathbf{E} = \frac{1}{\tau}\mathbf{g}(\mathbf{k})\cdot\mathbf{k} + C''\int_{\varphi'}(\mathbf{g}(\mathbf{k})\cdot\mathbf{k} - \mathbf{g}(\mathbf{k}')\cdot\mathbf{k}')\,|\langle\mathbf{k}'|\Delta U|\mathbf{k}\rangle_2|^2 d\varphi' \tag{3-50}$$

where C'' is again material and physical constant, and the integral equation is now posed for unknown function $g(\mathbf{k})\cdot\mathbf{k}$ instead of the original distribution function $f(\mathbf{k})$. The result is given by

$$\mathbf{g}(\mathbf{k})\cdot\mathbf{k} = -e\tau\mathbf{E}\cdot\mathbf{k} - C''\tau^2 e\int_{\varphi'}\mathbf{E}\cdot\mathbf{K}\,|\langle\mathbf{k}'|\Delta U|\mathbf{k}\rangle_2|^2 d\varphi' \tag{3-51}$$

or

$$\mathbf{g}(\mathbf{k})\cdot\mathbf{k} = -e\tau\mathbf{E}\cdot\mathbf{k}$$

$$-C''\tau^2 e\int_{\varphi'}\mathbf{E}\cdot\mathbf{K}K_y^2\left[\frac{1}{(\gamma K_x)^2+K_y^2} - \frac{2}{\gamma+1}\frac{1}{K_x^2+K_y^2+\alpha}\right]^2 d\varphi' \tag{3-52}$$

where the performance of Fourier transformation on the two dimensional perturbation potential, ΔU, leads the last equation 3-52. (APPENDIX B)

III-2-2. Electrical Resistivity

By making use of the solution of B.T.E. obtained above, electrical resistivity is calculated. The calculation is started with the following definition of electron flux, J.

$$\mathbf{J} = -\frac{e}{4\pi^3}\int\int\int_{\mathbf{k}} \mathbf{v}_{\mathbf{k}} f(\mathbf{k}) d\mathbf{k} \tag{3-53}$$

or

$$J_i = -\frac{e}{4\pi^3}\int\int\int_{\mathbf{k}} v_i f(\mathbf{k}) d\mathbf{k} \quad (i = x, y, z) \tag{3-54}$$

Substitution of the eq. 3-49 into the eq. 3-54 followed by the applications of the eq. 3-40 and the next properties of equilibrium distribution function

$$\int\int\int e v_i f^0 d\mathbf{k} = 0 \tag{3-55}$$

and

$$\frac{\partial f^0}{\partial \varepsilon} \cong -\delta(\varepsilon - \varepsilon_F) \tag{3-56}$$

yields

$$J_i = -\frac{e}{4\pi^3}\left[\frac{\hbar}{m}\right]^2 \int\int\int_{\mathbf{k}} k_i \mathbf{g}(\mathbf{k})\cdot\mathbf{k}\delta(\varepsilon - \varepsilon_F) d\mathbf{k}$$

$$= -\frac{e}{4\pi^3}\left[\frac{\hbar}{m}\right]^2 \int\int_{S_{\varepsilon_F}} \frac{k_i}{\hbar v_i} \mathbf{g}(\mathbf{k})\cdot\mathbf{k} d\mathbf{k} S_{\varepsilon_F} \quad (i = x, y, z) \tag{3-57}$$

where the reduction of the integral is again based on the same procedures introduced previously in the eq. 3-39. It should be noticed that, in contrast to the universality of the condition 3-55, the eq. 3-56 is the approximate relation except for absolute zero Kelvin. This point is discussed in the next chapter IV-3.

Electrical resistivity (conductivity) is essentially expressed as a tensor and each component, J_x, J_y, J_z, in the eq. 3-57 is responsible for those tensor components. Mathematical extraction of the resistivity (conductivity) tensor components from the electron flux J is demonstrated below for the case of $i=x$ ie.

J_z. By substituting the eq. 3-40 into the eq. 3-57 and by making a coordinate transformation from the Cartesian system to the Polar system, the next equation is obtained.

$$J_z = -\frac{3en_0}{4\pi mk_F}\int_{\vartheta}\int_{\varphi} \mathbf{g}(\mathbf{k})\cdot\mathbf{k}\sin^2\vartheta\cdot\cos\varphi\cdot d\vartheta d\varphi \tag{3-58}$$

where the geometrical relation among ϑ,φ and k_F are given in the Fig. 5, and n_0 is the electron density of perfect crystal which is related with Fermi vector, k_F, by

$$n_0 = \frac{k_F^3}{3\pi^2} \tag{3-59}$$

Substitution of the eq. 3-52 into the eq. 3-58 yields two integrals.

$$\begin{aligned} J_z &= J_z^{(1)} + J_z^{(2)} \\ &= -A\sigma\tau\int_0^{\pi} d\vartheta \int_0^{2\pi} d\varphi E_z k_z \sin^2\vartheta\cdot\cos\varphi \\ &\quad -AC''\sigma\tau^2\int_0^{\pi} d\vartheta \int_0^{2\pi} d\varphi \int_0^{2\pi} d\varphi' E_z K_z F(K_x,K_Y)\sin^2\vartheta\cos\varphi \end{aligned} \tag{3-60}$$

where A and $F(K_x,K_y)$ are given by

$$A = -\frac{3en_0}{4\pi mk_F} \tag{3-61}$$

and

$$F(K_x,K_y) = K_y^2\left\{\frac{1}{(\gamma K_x)^2+K_y^2} - \frac{2}{\gamma+1}\frac{1}{K_x^2+K_y^2+\alpha}\right\}^2 \tag{3-62}$$

Since the conductivity tensor (inverse of the resistivity), Ω, is defined as

$$\mathbf{J} = \Omega \mathbf{E} \tag{3-63}$$

the tensor component $\sigma_{xx}^{(1)}$ can be singled out from $J_x^{(1)}$.

$$\sigma_{xx}^{(1)} = -Ae\tau \int_0^{\pi} d\vartheta \int_0^{2\pi} d\varphi k_F \sin^2\vartheta \cos\varphi$$

$$= \frac{n_0 e^2 \tau}{m} \tag{3-64}$$

In the same manner, although the calculation is complicated, $\sigma_{xx}^{(2)}$ is obtained from $J_x^{(2)}$.

$$\sigma_{xx}^{(2)} = -AC^{**} e\tau^2 \int_0^{\pi} d\vartheta \int_0^{2\pi} d\varphi \int_0^{2\pi} d\varphi' K_x F(\mathrm{K}) \sin^2\vartheta \cdot \cos\varphi$$

$$= -AC^{**} e\tau^2 k_F C^{**} \pi^2 \left\{ 2 + \left[\frac{\Gamma_0}{1-\Gamma_0} \right]^2 \frac{p^2}{1+p^2} + p \frac{\Gamma_0(4-3\Gamma_0)}{(1-\Gamma_0)^2} \sin^{-1} \frac{1}{\sqrt{p^2+1}} \right\} \tag{3-65}$$

where C^{**}, p and Γ_0 are given by

$$C^{**} = -\frac{2(1-\Gamma_0)^2}{2^2 k_F^3 (\gamma^2)^2} \tag{3-66}$$

$$p = \frac{\sqrt{a}}{2k_F} \tag{3-67}$$

and

$$\Gamma_0 = \frac{2\gamma^2}{1+\gamma} \tag{3-68}$$

From the first line to the second one in the eq. 3-65, the following assumption was employed,

$$\gamma \sim 1 \tag{3-69}$$

of which validity is discussed later. For the other components, y and z, the

same manipulations lead to the following results.

$$\sigma_{yy}^{(1)} = \sigma_{zz}^{(1)} \tag{3-70}$$

$$\sigma_{yy}^{(2)} = 3\sigma_{zz}^{(2)} \tag{3-71}$$

$$\sigma_{xx}^{(1)} = \sigma_{zz}^{(1)} \tag{3-72}$$

and

$$\sigma_{xx}^{(2)} = 0 \tag{3-73}$$

The final step is an elegant applications of the Matthiesen's rule [32]. According to the Matthiesen's rule the resistivity is given as the sum of two contributions. One is the contribution of lattice vibration which depends on temperature and the other one is caused by impurities, defects and so on which is generally independent of temperature. Thus, mathematically, this rule is described by

$$\frac{1}{\sigma_{zz}} = \frac{1}{\sigma_l} + \frac{1}{\sigma_z} \tag{3-74}$$

where the first term of the right hand side is the resistivity of lattice and the second one is that of the dislocation which is the final object of this calculation. σ_l is easily derived from fundamental solid state electronics [33] and is given by

$$\sigma_l = \frac{n_0 e^2 \tau}{m} \tag{3-75}$$

One would notice that this is nothing more than $\sigma_{zz}^{(1)}$,$\sigma_{yy}^{(1)}$ and $\sigma_{xx}^{(1)}$ obtained above. Here the following assumption is introduced; the lattice contribution is much greater than that of the dislocation.

$$\sigma_l \ll \sigma_z \quad \text{ie.} \quad \frac{1}{\sigma_l} \gg \frac{1}{\sigma_z} \tag{3-76}$$

Then, from eq. 3-74, σ_{zz} is approximated to be

$$\sigma_{zz} \sim \sigma_i - \frac{\sigma_i^2}{\sigma_z} \tag{3-77}$$

and by making use of the above eq.3-77 with

$$\sigma_{zz} = \sigma_{zz}^{(1)} + \sigma_{zz}^{(2)} \tag{3-78}$$

and

$$\sigma_{zz}^{(1)} = \sigma_i \tag{3-79}$$

the dislocation resistivity, ρ_z, can be extracted.

$$\rho_z = \frac{1}{\sigma_z}$$

$$= -\frac{\sigma_{zz}^{(2)}}{(\sigma_{zz}^{(1)})^2} \tag{3-80}$$

Likewise

$$\rho_y = 3\rho_z \tag{3-81}$$

and

$$\rho_x = 0 \tag{3-82}$$

Although substitution of eqs.3-64 and 3-65 makes the above equation more realistic, this task is accomplished in the next chapter.

III-3. Friction Force.

In the previous section it was demonstrated that a moving edge dislocation line causes electrical resistivity as an intrinsic property. On the other hand,

during the motion with velocity v, the dislocation experiences the electric current, i, caused by positive ion charges. As a result Joule heat energy is expected to be dissipated. This energy should be supplied externally in order to keep the steady motion. The friction force on a moving edge dislocation originates from this energy loss and is estimated in the following manner.

The configuration in the Fig. 6 is considered. According to the well known Joule-Lenz Law, the heat energy dissipated by the current i, in an object of resistivity R, during time t, is given by

$$Q_{heat} = i^2 R t$$

$$= i^2 \rho \frac{L_0}{A_0} t \tag{3-83}$$

The electric current, i, experienced by the dislocation of velocity, v, is

$$i = e n_0 A_0 v \tag{3-84}$$

where A_0 is the transverse area of the model sample shown in the Fig. 6, and is given by

$$A_0 = Wh \tag{3-85}$$

and time, t, is also easily calculated.

$$t = \frac{L_0}{v} \tag{3-86}$$

Substitution of the eqs. 3-84~3-86 into the eq. 3-83 yields

$$Q_{heat} = e^2 n_0^2 v \rho L_0^2 A_0 \tag{3-87}$$

Let F' be the applied force on a dislocation of unit length to keep the steady motion, which is equivalent to the friction force. Then the following relation is

obtained.

$$F^* L_0 = Q_{heat} \tag{3-88}$$

And from eqs. 3-87 and 3-88, the friction force per unit length is estimated to be

$$F^* = e^2 n_0^2 v \rho \tag{3-89}$$

By substituting the previously obtained results of electrical resistivity and the appropriate physical constants into the eq. 3-89, the friction force is explicitly obtained as

$$F^* = 5.07\times10^{8}\left\{b^2\left[\frac{v_s}{v_l}\right]^4 v_l\right\}G^*(p,\gamma) \tag{3-90}$$

and

$$G^*(p,\gamma) = \frac{\sqrt{1-\gamma^2}}{(\gamma)^2}\frac{1}{p^{10}}\left[2(1-\Gamma_0)^2+\Gamma_0\frac{p^2}{p^2+1}+p\,\Gamma_0(4-3\Gamma_0)\sin^{-1}\frac{1}{\sqrt{p^2+1}}\right] \tag{3-91}$$

where p and Γ_0 were given in the eqs. 3-67 and 3-68.

III-4. Magnetic Induction

Magnetic induction is the dynamic effect of moving charges. In a strict manner, it should be derived as the solution of the Maxwell's equations 2-28~2-31. In this study, however, all the treatments so far have been limited to the quasi-statical treatment in which the vector potential is ignored and the problem is posed as the effect of "moving electrostatic potential". Then, within the frame work of this model, the following results are not expected to satisfy Maxwell's equations rigorously and the calculation itself may not be compatible with the model. In spite of this basic refutation, however, it is still considered

to be of consequence to estimate the magnetic induction because of the following two reasons. First of all, the results will provide the limitation of the quasi-static treatment: if the estimated magnetic induction is not negligibly small, the spatial density of electrons which was given by the eq. 3-19 should be modified by returning to Maxwell's equations so that the vector potential is incorporated in the model. Secondly, the possibility of a new type of interaction between the magnetic field around a moving dislocation and the magnetic moments of magnetic ion clusters in the crystal can be examined.

The procedure adopted here is rather simple and straightforward. The basic origin of the magnetic induction is the motion of the electron cloud associated with the moving dislocation line. Instead of applying the full expression of the electron density eq. 3-19, the limiting case of infinite screening constant, $\sqrt{\alpha^*}=\infty$, is calculated.

The magnetic induction caused by a moving charge, Q_{charge}, is generally given by

$$B = |\mathbf{B}| = \frac{\mu_0}{4\pi} \frac{Q_{charge} v}{r^2 \left(1-\frac{v^2}{c^2}\right)^{\frac{1}{2}}} \tag{3-92}$$

where μ_0 is the permeability constant and r is the distance between the charge Q_{charge} and an observing point. As mentioned before, the speed of a dislocation, v, is very much smaller than that of light, c. Therefore, the above equation can be approximated as

$$B \sim \frac{\mu_0}{4\pi} \frac{Q_{charge} v}{r^2} \tag{3-93}$$

A more general vector description of the magnetic induction for the moving charge in the x-direction is given by

$$\mathbf{B} = B_i |e_i> \quad (i=x,y,z)$$

$$= -\frac{\mu_0 v Q_{charge}}{4\pi r^3} r_z |e_y> + \frac{\mu_0 Q_{charge} v}{4\pi r^3} r_y |e_z> \tag{3-94}$$

where B_i and $|e_i>$ are the component of the magnetic induction and the unit vector in the i-direction, respectively. For simplicity the present calculation is performed only on the $x-y$ plane on which the B_y component vanishes because of the symmetry of the charge distribution, and only the B_z component

$$B_z = \frac{\mu_0 Q_{charge} v}{4\pi r^3} r_y \tag{3-95}$$

remains.

By applying this elementary principle to the moving electron cloud associated with the edge dislocation, the following calculation is carried out. The induction, ΔB_z, at the position $P(x,y,0,t)$ caused by the electron clouds residing in the volume element $(x'_i+\Delta x'_i, y'_j+\Delta y'_j, z'_k+\Delta z'_k)$ is given by

$$\Delta B_z(x'_i, y'_j, z'_k, t)$$

$$= \frac{\mu_0 v}{4\pi} \frac{y-y'_j}{\{(x-x'_i)^2+(y-y'_j)^2+(z'_k)^2\}^{3/2}} \frac{(-e)C_1 \gamma y'_j}{\{(x'_i-vt)^2+(\gamma y'_j)^2\}} \Delta x'_i \Delta y'_j \Delta z'_k \tag{3-96}$$

where the second fraction term expresses the space term, $\frac{r_y}{r^3}$, in the eq. 3-94, the third fraction term is the electron density which is calculated in eq. 3-19 and C_1 is the physical constant given by

$$C_1 = -\frac{b}{15}\frac{1}{\pi^3}\left(\frac{2m}{\hbar^2}\right)^{3/2}\left[\frac{1-2\nu_0}{1-\nu_p}\right]\varepsilon_F^{03/2} \tag{3-97}$$

Then the final formula for the magnetic induction $B(x,y,0,t)$ is obtained by integrating the eq. 3-96 over the crystal in the following way.

$$B_z(x,y,0,t) = \lim_{\Delta x_i', \Delta y_j', \Delta z_k' \to 0} \sum_i \sum_j \sum_k \Delta B_z(x_i', y_j', z_k', t) \Delta x_i' \Delta y_j' \Delta z_k'$$

$$= -\frac{e\mu_0 v}{4\pi} C_1 \gamma \int\int\int \frac{y - y'}{\{(x-x')^2 + (y-y')^2 + (z-z')^2\}^{3/2}} \frac{y'}{(x'-vt)^2 + (\gamma y')^2} dx' \cdot dy' \cdot dz' \tag{3-98}$$

The actual integration of the above eq. 3-98 was performed numerically after the reduction of the triple integral to the single integral.

IV. RESULTS AND DISCUSSION

IV-1. Electron Density and Perturbation Potential

In the former chapter, the electrostatic potential was obtained in eq. 3-16 with the Green's function $g_2(\mathbf{r}|\xi)$, and the third term could be neglected by the numerical evaluation. This numerical process is briefly examined before the discussion of the physical significance of the calculated electron density and electrostatic potential.

By excluding the common constant term from each term, the electrostatic potential, $\varphi(\mathbf{r})$, is given by the sum of three terms.

$$\varphi(\mathbf{r}) = -\frac{D}{\alpha}(\Delta(\mathbf{r}) - 2C\sqrt{\alpha}K_1(\sqrt{\alpha}\,|\mathbf{r}|)\frac{\sin\vartheta}{\gamma+1} + \int\int_{\mathbf{R}_2} g_2(\mathbf{r}|\xi)\nabla^2\Delta d\xi) \tag{3-16}$$

$$= -\frac{D}{\alpha}C(I_1+I_2+I_3) \tag{4-1}$$

where

$$I_1(x,y) = \frac{\gamma y}{x^2+(\gamma y)^2} \tag{4-2}$$

$$I_2(x,y) = \frac{2\sqrt{\alpha}}{\gamma+1}K_1(\sqrt{\alpha}\sqrt{x^2+y^2})\frac{y}{\sqrt{x^2+y^2}} \tag{4-3}$$

$$I_3(x,y) = \frac{\gamma(1-\gamma^2)}{\pi}\int\int_{\mathbf{R}_2} K_0(\sqrt{\alpha}\,|\mathbf{r}-\xi|)\frac{\xi_y(3\xi_x^2-\gamma^2\xi_y^2)}{(\xi_x^2+\gamma\xi_y^2)^3}d\xi_x d\xi_y \tag{4-4}$$

Each contribution was plotted in Figs. 2, 3, and 4 for various points (x',y'). The employed velocities are $0.25v_l$(γ=0.968) and $0.5v_l$(γ=0.865) which is the possible maximum velocity, and the screening constant, $\sqrt{\alpha}$, is fixed at 1.5×10^8. (The validity of this adopted value of screening constant is demonstrated in the discussion, eq. 4-15.) It can be clearly seen that the essential contribution is

attributed to the first term both for the diagonal direction and on the circle, and the magnitude of the third term is significantly smaller than those of other terms. In the light of these numerical results the third term was neglected in the calculation procedures. Although the physical meaning of this term is still open to question, it should be noticed that the dilatation, Δ, becomes a harmonic function for a static dislocation and therefore the third term spontaneously vanishes. This fact implies that the third term represents a dynamic effect. Probably strict solution of the Maxwell's equations will settle this ambiguity satisfactorily.

Now attention is turned to the calculated electron density. The eq. 3-19 is split into two terms and the physical meaning of each term is considered.

$$\rho(\mathbf{r}) = \rho_0\left[1-\Delta+\frac{4}{5}C\sqrt{\alpha}K_1(\sqrt{\alpha}\,|\mathbf{r}|)\frac{\sin\vartheta}{\gamma+1}\right] \tag{3-19}$$

$$= \rho_1(\mathbf{r})+\rho_2(\mathbf{r}) \tag{4-5}$$

where

$$\rho_1(\mathbf{r}) = \rho_0(1-\Delta) \quad \Delta \ll 1 \tag{4-6}$$

$$\cong \rho_0(1+\Delta)^{-1} \tag{4-7}$$

and

$$\rho_2(\mathbf{r}) = \rho_0\left[\frac{4}{5}C\sqrt{\alpha}K_1(\sqrt{\alpha}\,|\mathbf{r}|)\frac{\sin\vartheta}{\gamma+1}\right] \tag{4-8}$$

Since $(1+\Delta)^{-1}$ expresses the lattice dilatation the first term, $\rho_1(\mathbf{r})$, indicates the electron density whose shift is accompanied with positive ions on the lattice points. In this sense these electrons are tightly bound to the positive ions like

an ionic crystal. The essential feature of a metal is reflected in the second term, $\rho_2(r)$, which is the contribution of the screening effect of free electrons. In order to show these two effects schematically, the following modifications are performed on the eq. 3-13. The dilatation, Δ, was given by

$$\Delta = C\frac{\gamma y}{x^2+(\gamma y)^2} \tag{4-9}$$

where

$$C = \left[-\frac{b}{2}\pi\right]2\left\{\frac{v_s}{v_l}\right\}^2 \tag{3-17}$$

Then the eq. 3-19 is rewritten as

$$\frac{\rho(r)-\rho_0}{\rho_0 C^*} = \frac{\gamma y}{x^2+(\gamma y)^2} - \frac{4}{5}\frac{1}{\gamma+1}\sqrt{a}\sqrt{x^2+y^2}K_1(\sqrt{a}\sqrt{x^2+y^2})\frac{y}{x^2+y^2} \tag{4-10}$$

where

$$C^* = -C \tag{4-11}$$

The eq. 4-10 describes the change of the density rather than density itself. The screening term $\sqrt{a}$ was more explicitly given by eq. 3-12.

$$a = \frac{8\pi e^2\rho_0}{\varepsilon^0_{kin}} \tag{3-12}$$

$$= 1.969\times e^2\frac{2m}{\hbar^2}\rho_0^{\frac{1}{3}} \tag{4-12}$$

and has the dimension $[L^{-1}]$. Substitution of appropriate physical constants into the above equation yields,

$$a = 7.496\times10^8\rho_0^{\frac{1}{3}}\ [\text{c.g.s.}] \tag{4-13}$$

Since the electron density, $\rho_0(=n_0)$, of a typical metal resides in the range of

$$10^{22} \leq \rho_0 \leq 2\times10^{23} \tag{4-14}$$

the screening constant is confined to the following range.

$$1.616\times10^{16}\,[cm^{-1}] \leq \alpha \leq 4.386\times10^{16}\,[cm^{-1}] \tag{4-15}$$

The performance of the following scaling

$$\begin{aligned} x\ [cm] &= 10^{-8} X\ [angstrom] \\ y\ [cm] &= 10^{-8} Y\ [angstrom] \\ \sqrt{\alpha}\ [cm^{-1}] &= 10^{8}\sqrt{\alpha^*}\ [angstrom^{-1}] \end{aligned} \tag{4-16}$$

transforms eq. 4-10 into the final desired form.

$$\frac{\rho(r)-\rho_0}{\rho_0 C^* 10^8} = \frac{\gamma Y}{X^2+(\gamma Y)^2} - \frac{4}{5}\frac{1}{\gamma+1}\sqrt{\alpha^*}\sqrt{X^2+Y^2}K_1(\sqrt{\alpha^*}\sqrt{X^2+Y^2})\frac{Y}{X^2+Y^2} \tag{4-17}$$

The contributions of the first term, the second term and the whole term are schematically plotted in Figs. 7, 8, 9 and 10 for various values of γ and $\sqrt{\alpha^*}$. (Since the first term is independent of the screening constant, $\sqrt{\alpha^*}$, the contribution of this term is shown as the function of three values of velocities, v/v_t=0.0, 0.25 and 0.5 in the Fig. 7. The dependencies of the second term and whole term on three types of screening constant, $\sqrt{\alpha^*}$ = 1.0, 1.5, 2.0, are plotted in the Figs. 8, 9, and 10, respectively, for the three kinds of velocities. "GM" and "SCR" in each figures stand for γ and $\sqrt{\alpha^*}$. Scales are units of Burgers vector.) The dark part indicates a higher electron density than the light part. It is immediately understood that the screening contribution is a localized effect and that total electron density is determined primarily by the first term, which is nothing more than the equivalent consequence of the former calculations of

electrostatic potential given in the eqs. 4-2~4-4. One should notice that the electron density is antisymmetric with respect to x-axis and blows up at the origin. This explosion at the origin is observed in the electrostatic potential as well and therefore in the perturbation potential as is shown in the Figs. 11, 12 and 13. The origin of this physically unallowable phenomenon is the direct consequence of the application of linear elasticity argument to the core portion, which was introduced in the section II-2. It is well recognized that the atomic arrangement of the core can not be predicted by the linear elasticity theory. There might be some relaxation process in the core and there must be more suitable smooth function which describes the real strain or dilatation in the core portion. Since progress has been gradually made in the field of "core physics" mainly based on computer simulation study [34] and quantum mechanical approaches[35], the improvement and modification of the core portion by applying non-elasticity arguments remains as indispensable task in the future.

IV-2. Born Approximation

The Born approximation (APPENDIX A) adopted in this calculation is one of the typical classical treatments of perturbation theory. In this treatment, the wave function of the corresponding perturbed Hamiltonian is approximated to that of the perfect system, and only "small" perturbation potentials can be well described by this theory. In the present study, magnitude of the perturbation potential given by eq. 3-35 is about $6.4\times10^{-3}\varepsilon^{0}_{kin}$ at $(5b, 5b)$ for the case of $k_p=1.5\times10^{8}, b=3.0$Å and $\gamma=0.1$. This value may be fairly small enough to satisfy the criterion of the Born Approximation. However, as shown in the Fig. 11, perturbation potential blows up approaching toward the origin. Therefore the direct application of the Born Approximation to a whole crystal must be open to

objections. There could be a more suitable treatment for this type of strong scattering potential field. But the essential point is not the improvement or modification of the approximation method but to obtain the proper scattering potential field based on the proper atomic arrangement in the core portion.

IV-3. Boltzman Transport Equation and Mackenzie-Sondheimer's procedures.

The key procedure of the Mackenzie-Sondheimer's B.T.E. method is the dextrous application of the Matthiesen's rule in the final stage. It is not too much to say that the mathematical elegance of the whole method is amplified by this procedure. This powerful method, however, includes the following self-contradiction. The final process to obtain the resistivity value was based on the assumption;

$$\sigma_i \ll \sigma_s \quad i.e. \quad \frac{1}{\sigma_i} \gg \frac{1}{\sigma_s} \tag{3-76}$$

which means the resistivity of the lattice is very much higher than that of the dislocation. Since the relaxation time τ of lattice resistivity decreases inversely proportional to the temperature and according to Matthiesen's rule the resistivity of dislocations is independent of temperature, the assumption eq. 3-76 should describe the higher temperature state. On the other hand, once returned to the reduction process from eq. 3-54 to eq. 3-67, one realizes that the mathematical property of the Fermi-Dirac distribution function, eq. 3-56, was an essential ingredient. But this functional property is, in a rigorous sense, limited to 0^0K. This self-contradiction seems to violate the physical validity of this method.

In order to extract the pure contribution of a dislocation at 0^0K, the numerical calculation was carried out on the following integral equation 4-18 which is obtained from eq. 3-48 in the limit of infinite relaxation time (The

mathematical detail is shown in the APPENDIX C.)

$$-e\,\mathbf{k}\cdot\mathbf{E} = C'\int_{\varphi'}(g(\mathbf{k})\cdot\mathbf{k}-g(\mathbf{k}')\cdot\mathbf{k}')\,|\langle\mathbf{k}'|-e\varphi|\mathbf{k}\rangle_2|^2 d\varphi' \qquad (4\text{-}18)$$

Comparison of the numerical results with analytical results is made in the Table 1 for the case of a static dislocation, γ=1, and $\sqrt{a^2}$=1.5. (In Table 1, coefficient term is omitted and only k_F-dependent values are listed.) It can be understood that, although the analytical values are slightly higher than the numerical values which give the real dislocation resistivity, the Mackenzie-Sondheimer's analytical procedures provides a fairly good estimation of dislocation resistivity. The origin of this good agreement can be attributed to the following functional property of the Fermi-Dirac distribution function: The Fermi-Dirac distribution function is an exact step function at 0^0K, and deviation from the step function is negligibly small even at the higher temperatures. This guarantees the validity of the eq. 3-56 in the wide temperature range.

IV-4. Friction Force and Electrical Resistivity

The theoretical friction force was given by the eqs. 3-90 and 3-91.

$$F^* = 5.07\times10^8\left\{b^2\left[\frac{v_s}{v_t}\right]^4 v_t\right\}G^*(p,\gamma) \qquad (3\text{-}90)$$

$$G^*(p,\gamma) = \frac{\sqrt{1-\gamma^2}}{(\gamma^2)^2}\frac{1}{p^{10}}\left\{2(1-\Gamma_0)^2+\Gamma_0\frac{p^2}{p^2+1}+p\,\Gamma_0(4-3\Gamma_0)\sin^{-1}\frac{1}{\sqrt{p^2+1}}\right\} \qquad (3\text{-}91)$$

These results are plotted in the Fig.14 as a function of velocity for various values of Fermi vector, k_F [36]. It is understood that damping constants which can be calculated from the slope of the curve is, in general, a function of velocity. However, as shown in the Fig. 15, force is linearly related with velocities for their physically meaningful values. And damping constant is independent of

velocity. In order to estimate the actual values predicted by this theoretical calculation, physical and materials constants which are tabulated in the Table 2 are substituted into the above equations, and damping constants are estimated for Cu, Pb, and Al. The results are tabulated in the Table 3. It is needless to say that the accuracy of these values and the validity of the theory can be examined only by comparison with the experimental values. However, it is not an easy task to experimentally extract the friction force and damping constant with accuracy sufficient enough to allow comparison with theoretical values. A sample should not have high Peierls potential field so that the free flight dislocation motion is a dominant mode, and the temperature should be low enough to avoid the phonon friction force. In the case of a tensile test, in addition to these requirements for the sample and experimental condition, a more essential difficulty arises in the following manner.

A tensile test is one of the most widely used experimental procedures for the mechanical testing of materials. In fact, as was mentioned previously, the existence of the electron friction force was first predicted by this type of experiment. But in order to obtain the friction force from the observed stress change due to the superconducting and normal transition, the following theoretical procedures are required. The strain rate of a sample, $\dot{\varepsilon}$, is generally given by

$$\dot{\varepsilon} = N_m b \bar{v} \tag{4-19}$$

where N_m is the mobile dislocation density, $\bar{v}$ is the average velocity of those dislocations and b is the magnitude of the Burgers vector. When the rate controlling process is assumed to be a thermally activated process the velocity can be rewritten as

$$\bar{v} = \frac{L_a}{t_w} \tag{4-20}$$

$$= L_s \nu \exp\left[-\frac{\Delta G^*}{kT}\right] \tag{4-21}$$

where ΔG^* is the activation free energy; L_s is the average distance among obstacles; ν is the trial frequency and t_w is the waiting time for the thermal activation at an obstacle. The activation free energy can be more explicitly given by

$$\Delta G^* = G_0 - (\tau_{app} - \tau_L) V_{act} \tag{4-22}$$

where G_0 is the interaction energy between a dislocation and an obstacle; τ_{app} and τ_L are the applied force and long range internal back stress due to other dislocations, respectively, and V_{act} is the activation volume. Substitution of the eqs. 4-21 and 4-22 into the eq. 4-19 yields

$$\dot{\varepsilon} = N_m b L_s \nu \exp\left[-\frac{G_0 - (\tau_{app} - \tau_L) V_{act}}{kT}\right] \tag{4-23}$$

From the above equation, the applied stress, τ_{app}, can be obtained as

$$\tau_{app} = \tau_L + \frac{G_0}{V_{act}} - \frac{kT}{V_{act}} \ln\left[\frac{\dot{\varepsilon}}{N_m b L_s \nu}\right] \tag{4-24}$$

By performing this procedure on both the normal and superconducting states, and by assuming that the long range internal stress, activation volume and mobile dislocation density do not change with the transition, the observed stress change due to the transition can be described by the following quantities.

$$\Delta\tau = (\tau_{app})^n - (\tau_{app})^s \tag{4-25}$$

$$= (\tau_e)^n - (\tau_e)^s \tag{4-26}$$

where superscript n and s indicate the normal and superconducting states, respectively. Since the electron friction force τ_e can be related with the

damping constant B_e and the velocity v by

$$\tau_e = \frac{B_e v}{b} \tag{4-27}$$

the eq. 4-26 can be rewritten as

$$\Delta\tau = \frac{v}{b}(B_e^n - B_e^s) \tag{4-28}$$

$$= \frac{v}{b} B_e^n (1-\Gamma) \tag{4-29}$$

where Γ is

$$\Gamma = \frac{B_e^s}{B_e^n} \tag{4-30}$$

$$= \left[\frac{T}{T_c}\right]^4 \quad (two\ fluid\ model) \tag{4-31}$$

or

$$= \frac{2}{1+\exp(\Delta_g / kT)} \quad (B.C.S.\ theory) \tag{4-32}$$

Then, as the product of damping constant B and velocity v, the electron friction force in the normal state, Fe^n, can be obtained from the eq. 4-29,

$$F_e^n = B_e^n v$$

$$= \frac{b}{1-\Gamma}\Delta\tau \tag{4-33}$$

or from eqs. 4-28 and 4-30, Fe^s is

$$F_e^s = B_e^s v$$

$$= \frac{\Gamma}{1-\Gamma} b \Delta\tau \qquad (4\text{-}34)$$

In the above calculations, the interaction force is obtained as only a function of temperature and measured stress change. However, this procedure is much too roundabout a process and many unclarified assumptions are piled up. In fact, there is no physical basis that can guarantee the assumption of invariability of the τ_L, G_0 or V_{act} between the two states. Estimation of the average distance L_s appeared in the eq. 4-23 belongs to the statistical problem of hardening which was introduced in chapter I-1. But the extension of the statistical problem of a static dislocation to that of a dynamic dislocation has not yet been satisfactorily investigated. Also, as was mentioned in chapter I-3, it is reported that, in the superconducting state, a dislocation which moves with a velocity higher than some critical velocity destroys the condensed electron pair and an additional friction force is exerted.[12] This microscopic physical property of the superconducting state is not taken into account in the above treatment. The effect of the magnetic field on the sample, which must be applied in order to pull the sample back to the normal state below critical temperature, is still open to question. Under the magnetic field, careless experimental alignment often does not make the testing machine behave as a mechanical reservoir. At any rate, even apart from these shortcomings, the most serious problem in the above treatment resides in the fact that raw data does not reflect the desired quantity directly and that the intervention of unclarified theories into the data interpretation process can not be avoided. Therefore one should conclude that it is next to impossible to extract a reliable value of a microscopic quantity such as the electron friction force from macroscopic values determined from a tensile test. In order to obtain reliable values of the friction force other experimental techniques must be sought.

Essentially three different approaches have been taken towards measuring the damping constant. One is the direct measurement of dislocation velocity as a function of applied stress by means of etch-pit technique; another one is the impact shear stress test which requires an assumption of a value for the mobile dislocation density; the other one is the measurement of ultrasonic attenuation. At this stage, it is recognized that the measurement of ultrasonic attenuation is the more reliable technique. The method proposed by Hikata et. al. [37] does not depend on a knowledge of the dislocation density and other inaccuracy resulting from dislocation networks. The details of their technique are not given here but their reported values of electron damping constant are tabulated in Table 3 with theoretical values including those obtained by present study. (Victoria et.al.'s measurement is based on impact shear tests.) Agreements between the values calculated in this work and the measured values are not excellent, but as a whole fairly good agreements are achieved.

Although it was mentioned that ultrasonic attenuation measurement was the most reliable available method, the obtained data must still be manipulated by theoretical calculations based on unfirmed assumptions. In this respect, the ultrasonic attenuation method is also an indirect measurement. By the way, as was demonstrated in the previous chapter, the essential physical basis behind this calculation was attributed to the Joule heat energy dissipation due to the electrical resistivity of a dislocation. Then, by digressing from the final calculation of friction force for a while, it is considered to be of great importance to focus on a comparison of the theoretical electrical resistivity value of a static dislocation with experimental values which can be much more directly measured than the friction force and, therefore, more reliable.

In order to select pertinent measured values of the resistivity for comparison, Matthiesen's rule is re-examined. This rule says that the electrical

resistivity, $\rho_d(N,T)$, due to N dislocations at temperature T is given by

$$\rho_d(N,T) = \rho_p(T) + \rho_d(N) \tag{4-35}$$

where $\rho_p(T)$ is the resistivity of pure crystal due to the lattice vibration and $\rho_d(N)$ is the contribution of N dislocations which does not depend on temperature. With the progress of measurement techniques, however, the existence of extra term, $\Delta\rho_{DMR}(N,T)$, such as

$$\rho_d(N,T) = \rho_p(T) + \rho_d(N) + \Delta\rho_{DMR}(N,T) \tag{4-36}$$

has been reported [38,39] and $\Delta\rho_{DMR}$ is named DMR (Deviation from Matthiesen's Rule). Since the construction of the present study is fully based on the Matthiesen's rule the experimental value which is compared with present theoretical results should not be affected by this uninvited DMR term. The main factors contributing to the DMR term are considered to be the development of cellular structures and the change of the phonon spectrum (vibration mode) due to the introduction of dislocations. Therefore, in order to eliminate DMR contributions, the experimental value should be selected from a sample which has a low dislocation density so that the lattice vibration mode is not very much perturbed, and has uniform distribution of dislocations without having substructures. Moreover, a low temperature measurement is required to suppress the lattice contribution, $\rho_p(T)$. To the author's knowledge, there is only one available experimental result which satisfies the above condition. This experiment was performed by Rider et. al. [40] on a poly Al crystal at liquid He temperature. In the Al sample, through the whole range of their measurement up to 15% strain, they observed a proportional relationship between resistivity and dislocation density (determined by TEM), and concluded that the additional contribution arising from configuration or density was avoided. Their measured

resistivity

$$\rho_{ex} = (1.8 \pm 0.1) \times 10^{-19} \quad [ohm-cm^3] \tag{4-37}$$

is adopted to compare with the present calculations whose general dependencies on velocities and Fermi vectors are shown in Fig. 16. Substitution of the material constants into the eqs. 3-64, 3-65, 3-80 and 3-81 followed by the modification for the poly crystal (APPENDIX D) yields

$$\rho_{th} = 1.02 \times 10^{-21} \quad [ohm-cm^3] \tag{4-38}$$

which is about two order lower than experimental value, ρ_{ex}, eq. 4-37. This theoretical value is slightly modified by the following corrections. According to the measurements and calculations of electronic specific heat, the effective mass of a conduction electron, m^*, in Al crystal is estimated to be

$$m^* = 1.48 m_0 \tag{4-39}$$

where m_0 is the static mass. Substitution of this relation into the eqs. 3-64~3-65 immediately makes small corrections on the calculated value, eq. 4-38.

$$\rho^* = 1.08 \rho \tag{4-40}$$

This is, probably, the theoretically highest obtainable estimation in this model. Although even this correction is not sufficient to fill the gap between the calculated and measured values this amount of discrepancy is not unexpected because of the following reason. Since the sample used was poly crystal there must be additional contributions of grain boundaries. The vacancies which are introduced during the deformation should add the extra contributions, as well. Then the experiment provides overestimated value as compared with the true contribution of dislocation itself.

Therefore one can conclude that this simple model gives a fairly good estimation of the resistivity. Moreover, as will be shown in the next section, the effect of the magnetic field -- the dynamic effect -- is negligibly small, then the model of friction force, which is simply extended as the quasi-static motion of charging cloud, can also provide the reliable estimation. And the result of eqs. 3-90 and 3-91 may be understood to be fairly reliable.

IV-5. Magnetic Induction and Magnetic Interaction

By substituting appropriate material and physical constants into the eqs. 3-97 and 3-98, the magnetic induction $B_z(x,y,o,t)$ is calculated as a function of dislocation velocity. In the Fig. 17, the spatial distribution of the integral part of the eq. 3-98 which depends only on the coordinates (x,y,z) , (x',y',z') and $\gamma(v)$ is shown for the case of v/v_1=0.3. In the Fig. 18, the same quantities are plotted as the function of y coordinates for the constant x value, $x=5b$, and three kinds of velocities. One can see that the magnetic induction blows up approaching to the origin; this has the same physical origin as the singularity observed for electron density or perturbation potential field. Substitution of the actual material constant into the above equation yields the magnitude of $10^{-35}\sim10^{-38}$ (Tesla/10^2b) for both Ag and Au on the radius of $5b$. These values are small enough to conclude that the effect of magnetic induction is virtually negligible.

As a very rough approximation, the magnitude of the magnetic interaction energy can be estimated, as well. The interaction energy between the magnetic induction, B, and the magnetic moment, μ, is given by [41]

$$E_{mag.} = \mathbf{B}\cdot\mu \qquad (4\text{-}41)$$

In the true sense, however, the magnetic induction B produced by the moving

dislocation is not independent but is varying with the dislocation motion. Then the interaction process with the "static" magnetic moment caused by a single atom, atomic cluster, short range ordering etc. in a crystal should be treated more strictly. In this respect, the above equation can not be applied directly to this problem, but as a first approximation the maximum interaction energy, $E_{mag.}^{max.}$, is calculated by the following equation.

$$E_{mag.}^{MAX.} = |B|_{MAX.} \cdot |\mu| \qquad (4\text{-}42)$$

where the magnetic moment is assumed to be parallel to the magnetic induction. Then by substituting the value of maximum induction on the radius of 5b and the Bohr magneton 10^{-23}J/Tesla into the above equation 4-42, the "magnetic interaction energy" $\sim 10^{-9}$ ev/b is obtained. This value is very much smaller than those of elastic or electric interaction energy.

The following two facts might be noticed in the above calculations. First of all, those calculations were carried out for the infinite screening constant which means non-screening effect. As was mentioned in the previous section, IV-1, the effect is not significant, and these estimations are expected not to be seriously modified. Secondly, the values of the magnetic induction on the radius of 5b were adopted for the above estimations. Within this radius, both the magnitude of induction and interaction energy are more magnified. However, without clear knowledge of core, those values should not be allowed to come into the estimation. Then the values on the assumed core radius 5b should be viewed as a possible estimation provided that from the outside core to the inside core physical values such as electron density are smoothly changing and, at the core radius, a maximum value appears.

The above discussion criticizes several unclear physics behind this calculation. But, as the very rough first estimation, one can conclude that both the

influence of the induced magnetic field (dynamic effect) on the previous calculation results and the possibility of magnetic interaction with a magnetic cluster are hardly expected.

IV-6. Possibility of The Extension to Many Body Problem (Collective Behavior of Dislocations) in Very Low Temperature Deformation

The main subject of this study has been the calculation of the interaction force between a single dislocation and the electrons. Most theoretical studies of very low temperature deformation behavior also have been concentrated on the single dislocation behavior. Even creep or stress relaxation phenomena, which can be observed even in the very low temperature region and should be essentially described by group behavior of dislocations, have been approached based on single dislocation behavior. Although, to some extent, those analyses have revealed the essence of the phenomena by introducing new interactions such as the dynamic effect or quantum effect, all explanations and predictions remain qualitative arguments because of the lack of knowledge of many body effects. The study of the interaction force between two dislocations for various type of configurations is certainly the important basic problem, but it is virtually impossible to apply the result to each single dislocation constituent and to analyze the macroscopic behavior even if a huge computer is available. Introduction of a thermodynamic treatment is essential. In this section, as one of many body problems, the possibility of obtaining the mobile dislocation density as a function of given deformation conditions such as temperature strain rate, damping constant and so on is discussed.

IV-6-1. Sumino Hypothesis

Historically, the many body problem was first discussed by Johnston and

Gilman [42], and they clearly clarified the dependency of the yielding behavior on various deformation factors. Haasen and Alexander's analysis [43] is also one of the typical examples of the many body problem. These treatments can reproduce the stress-strain curve under the given deformation condition. However, empirical equations are involved in the analysis. Moreover the physics behind many body effects are not well discussed. In this respect, one should say that these treatments are hybrid-theoretical treatments. On the other hand, Sumino et.al.[44,45] recently proposed a potentially useful hypothesis in the following way.

The strain rate $\dot{\varepsilon}$ was given by

$$\dot{\varepsilon} = N_m b \bar{v} \tag{4-19}$$

Mathematically, an infinite number of combinations of N_m and $\bar{v}$ are possible under a given strain rate $\dot{\varepsilon}$. However, this combination is not determined arbitrarily and there should be some physical principles which dominate the best combination of N_m and $\bar{v}$. Sumino et. al. proposed the following hypothesis to determine the combination. The steady state of moving dislocations is determined so as to make the component of the flow stress associated with moving dislocations the minimum necessary to maintain a given strain rate. The mathematical expression of the above hypothesis is given in the next equation.

$$\frac{\partial(\tau_{eff} + \tau_i^D)}{\partial N_m} = 0 \tag{4-43}$$

where τ_{eff} is the effective stress on a dislocation and τ_i^D is the interaction force among moving dislocations. The validity of this hypothesis has been reported to be proved for Ge and Si by their experiments [46]. And by applying the eq. 4-43, they successfully explained the dependency of the effective stress on strain rate and derived the equilibrium moving dislocation density as a function of

deformation conditions such as strain rate etc.. Moreover, based on irreversible thermodynamics, Nishioka [47] theoretically proved that this hypothesis is identical with the condition of the minimum rate of entropy production associated with plastic deformation.

Because of the simplicity of its mathematical statement, Sumino's analysis provides a great possibility of extension. However, there are two difficulties which should be overcome in its application to this study. One is the dynamic effects, ie. damping or inertia, which are not taken into account in their treatment. The other one is the difference of the mode of a dislocation motion. Their interest was focused on Ge and Si which have higher Peierls potential, and dislocation motion is characterized by the viscous mode. But in the case of dilute f.c.c. alloys, the Peierls potential is not high and obstacles are scattered point-wise;, then the dislocation motion is characterized as free flight motion [48]. (It is not too much to say that the existence of dynamic effects is limited to free flight motion and except for some anomalies arising from quantum tunneling through the high Peierls potential, most of the deformation anomalies at very low temperature are centered on f.c.c. alloys.)

IV-8-2. Extension to Free Flight Thermally Activated Motion with the Aid of Dynamic Effect

The above difficulties are overcome by the following modeling processes. The model schematically shown in the Fig.19 is considered and the following deformation parameters are initially introduced. N_m is the mobile dislocation density; b is the Burgers vector on this slip plane; c is the concentration of point obstacles; τ_{app} is the applied stress; τ_{eff} is the effective stress on a dislocation; B is the damping constant and the deformation temperature is T. In the case of viscous dislocation motion, the strain $\Delta\varepsilon$ during time Δt was given by

$$\Delta\varepsilon = N_m \cdot \Delta\bar{X} \cdot b \tag{4-44}$$

where $\Delta\bar{X}$ was the average displacement of mobile dislocations during time Δt. Then the strain rate $\dot{\varepsilon}$ was derived as

$$\dot{\varepsilon} = \lim_{\Delta t \to 0} \frac{\Delta\varepsilon}{\Delta t}$$

$$= \lim_{\Delta t \to 0} N_m \frac{\Delta\bar{X}}{\Delta t} b \tag{4-45}$$

$$= N_m \bar{v} b \tag{4-19}$$

This is quite a general and familiar formula for the strain rate. On the other hand, in the case of free flight motion, it should be modified in the following way. As the rate controlling process of a dislocation motion, thermally activated processes at an obstacle assisted by an inertia effect is assumed. This implies that the flight time between obstacles is negligible as compared with the captured time at an obst . the thermal activation is assumed to take place at ΔP obstacles per unit volume during time Δt. Then, the area, A_{swept},

$$A_{swept} = \Delta P (L_a)^2 \tag{4-46}$$

is swept away by dislocations and the strain, $\Delta\varepsilon$, per unit volume is given by

$$\Delta\varepsilon = \Delta P \cdot (L_a)^2 b \tag{4-47}$$

therefore strain rate is derived as

$$\dot{\varepsilon} = \lim_{\Delta t \to 0} \frac{\Delta\varepsilon}{\Delta t} \tag{4-48}$$

$$= \lim_{\Delta t \to 0} \frac{\Delta P}{\Delta t} (L_a)^2 b$$

$$= \dot{P}^{+}(L_s)^2 b \tag{4-49}$$

where L_s is the average distance among obstacles, and $(L_s)^2$ is the average area occupied by an obstacle. The most important assumption implied in eq. 4-46 is that, after overcoming an obstacle, a dislocation should be captured by the next obstacle it encounters. This assumption was originally made by Friedel [50] in his study of static dislocations and has been succeeded to following studies.

Let $\bar{L}$ be the average distance between obstacles along dislocations. Then the number of total points (obstacles) interacting with a dislocation is given by

$$P_T = \frac{N_m}{\bar{L}} \tag{4-50}$$

According to the thermal activation process developed by Suzuki [51] the waiting (captured) time at an obstacle, t_w, is

$$\frac{1}{t_w} = \nu \exp\left[-\frac{G_0 - bd\bar{L}\tau_{eff}\overline{Y_m}}{kT}\right] \tag{4-51}$$

where ν is the trial frequency, G_0 is the interaction energy between an obstacle and a dislocation, d is the width of an obstacle, and y_m is the parameter specifies the dynamic effect which is discussed later. The numerator of the exponent in the eq. 4-51 is the activation energy. Since $\dot{P}^{+}$ in the eq. 4-49 should be given by

$$\dot{P}^{+} = \frac{P_T}{t_w} \tag{4-52}$$

then substitution of eqs. 4-50 and 4-51 into the eq. 4-49 yields

$$\dot{\epsilon} = \left(\frac{N_m}{\bar{L}}\right)\nu \exp\left[-\frac{G_0 - bd\bar{L}\tau_{eff}\overline{Y_m}}{kT}\right] L_s^2 b \tag{4-53}$$

This is the final expression of the strain rate extended to the free flight mode of a dislocation motion.

The physical meaning of Y_m is discussed. As is shown in the Fig.20, the components of the line tension in the direction of dislocation motion, F_m, was given by

$$F_m = b\tau_{eff}\bar{L}Y_m \tag{4-54}$$

$$\overline{Y_m} = 1+0.6e^{-x^*} \tag{4-55}$$

and

$$x^* = \pi\gamma^*/\omega_0 \tag{4-56}$$

where γ^* and ω_0 were

$$\gamma^* = \frac{B}{2m} \tag{4-57}$$

and

$$\omega_0 = \pi\left(\frac{\Gamma}{m_d}\right)^{1/2}/\bar{L} \tag{4-58}$$

These quantities can be derived as the solution of the dislocation motion equation 1-1 of a string model. And Y_m which is multiplied by the static equilibrium force, $b\tau_{eff}\bar{L}$, can be viewed as the modification factor which specifies the dynamic effect. Since the vibration of dislocation is repeated many times, the dynamic effect due to the vibration should be incorporated to thermal activation process and the average value during the decay time $\frac{1}{\gamma^*}$ is inserted to the equation. Y_m in the eq. 4-54 is such an average value calculated by the following equation.

$$\overline{V_m} = 1+\frac{e^{-z^*}}{1/\gamma^*}\int_0^{\frac{1}{\gamma^*}} e^{-\gamma^* t}dt \tag{4-59}$$

$$\cong 1+0.6e^{-z^*} \tag{4-55}$$

This elaborate idea devised by Suzuki [12] seems to allow coexistence of the dynamic effect and the thermal activation process. However, thermal activation is essentially a statistical fluctuation phenomena, the deterministic dynamic term can not be accommodated in such a manner. The basic solution of this extremely hard problem might be settled by returning to basic physics [52]. In this study, Suzuki's method is adopted.

The average distance between obstacles along dislocations, $\bar{L}$, is generally a function of stress, line tension etc. and the search for the proper functional form belongs to the statistical problem of hardening. In the case of a static dislocation this problem has been almost worked out [53,54]. However, to the author's knowledge, nobody has succeeded in obtaining such a function for the general dynamic problem. Instead of going deeply into this problem, Friedel's statistics is applied under suitable assumptions. The traditional Friedel statistics tells that $\bar{L}$ can be related with stress, line tension and concentration of obstacle by the following equation.

$$\bar{L} = \left(2\frac{\Gamma}{bc}\right)^{\frac{1}{3}}\tau^{-\frac{1}{3}} \tag{4-60}$$

This relation was derived from the static force balance condition at an infinitesimal portion of a bowing arc and geometrical condition on the assumption that the area which is swept out by a dislocation between two obstacles is equal to the average area occupied by an obstacle. It should be noticed that

application of the Friedel's statistics immediately confine this problem to restricted condition: the vibration amplitude of a bowing string should not be very much deviated from static equilibrium configuration and, once overcoming an obstacle, a dislocation loses all memories about its dynamic vibration. In other words, the current overcoming process should not be influenced by previous processes. Moreover, unzipping effects can not be included. Substitution of the eq. 4-60 into the eq. 4-53 immediately yields

$$\dot{\varepsilon} = N_m \nu \left(\frac{b^4}{2\Gamma c^2}\right)^{\frac{1}{3}} \tau_{eff}^{\frac{1}{3}} \cdot \exp\left(-\frac{G_0 - bd\left(\frac{2\Gamma}{bc}\right)^{\frac{1}{3}} \tau^{\frac{2}{3}} \overline{Y_m}}{kT}\right) \tag{4-61}$$

and therefore

$$\Omega = \ln\tau_{eff} + \Phi(1+0.6e^{-\tau^*})\tau_{eff}^{\frac{2}{3}} \tag{4-62}$$

where

$$\Omega = 3\left\{\ln\frac{\dot{\varepsilon}}{N_m \nu\left(\frac{b^4}{2\Gamma c^2}\right)^{\frac{1}{3}}} + \frac{G_0}{kt}\right\}, \quad \Phi = \frac{3bd}{kT}\left(\frac{2\Gamma}{bc}\right)^{\frac{1}{3}} \tag{4-62'}$$

The final stage is the application of Sumino hypothesis to eq. 4-62. By assuming a suitable form of the interaction force between moving dislocations and the work hardening force, one would be able to describe the effective stress more concretely.

$$\tau_{eff} = \tau_{app} - \tau_i^0 - \tau_h \tag{4-63}$$

$$= \tau_{app} - A^* \sqrt{N_m} - \vartheta(\varepsilon - \varepsilon_a) \tag{4-64}$$

where τ_i^0 is the interaction force among moving dislocation and τ_h is caused by

static dislocations, namely the work hardening effect. But eqs. 4-83 and 4-84 are nothing more than assumptions. To obtain proper functional forms should be recognized as another important aspect of the many body problem. It will require very hard mathematical load to separate out τ_{eff} from the eq. 4-82 and it may not be able to be performed analytically. But by substituting eq. 4-84 into such a expression followed by an application of eq. 4-43, one will obtain the equilibrium (steady state) moving dislocation density, N_m^e, as a function of deformation condition. By substituting the electric damping constant obtained in the previous chapter eqs.3-90 and 3-91 into the, N_m^e, one can discuss the low temperature deformation phenomena more reliably as a further unified treatment. Those are possibilities and for future consideration.

V. CONCLUSIONS

As stated in the introduction, the primary goal of this study was to calculate the electron damping force in a normal state for a moving edge dislocation. Based on the free electron gas model, an equation which describes the electron friction force on a dislocation was analytically derived as a function of the normalized velocity of a dislocation and the Fermi vector. Damping constants which are determined from the force-velocity relations are generally a function of velocity. However, in the range of physically meaningful dislocation velocities, the force is linearly related to the velocity. Theoretical values of the damping constant obtained in this study shows fairly good agreements with experimental values. Electrical resistivity, as a middle product of this study, was compared with an experimental value for pure Al. The discrepancy is about an order of two. This discrepancy was ascribed to DMR sources of the sample. Also, direct numerical calculation was carried out to estimate the magnetic field associated with a moving dislocation. And the possibility of a magnetic interaction between a moving dislocation and local magnetic moments in a crystal was evaluated. The calculated magnetic field was negligibly small and any magnetic effects were hardly expected. Although ambiguity of core structure remains in the model, as a whole, this model provides fairly good estimations.

A possibility for a unified treatment of the three main dislocation problems, elementary interaction manner, statistical problem of hardening and collective behavior of dislocations, was discussed in the final section. And a fundamental equation, which may describe the essential features of deformation phenomena at very low temperatures, was derived. To solve the equation and to extend the model remain for future work.

Appendix A. Born-Approximation and Calculation of Scattering (Transition) Probability < I >

The time dependent Schrödinger equation can be given by

$$i\hbar\frac{\partial\Psi^0}{\partial t} = H^0\Psi^0 \tag{A-1}$$

where Ψ^o and H^o are the wave function and unperturbed Hamiltonian. The solution of above equation is easily found to be

$$\Psi_n^0 = \psi_n \exp\left[i\frac{E_n t}{\hbar}\right] \tag{A-2}$$

where ψ_n is space part of the wave function. Now, let us consider the perturbed system with perturbation potential, ΔU. The corresponding Schrödinger equation is given by

$$i\hbar\frac{\partial\Psi}{\partial t} = (H^0+\Delta U)\Psi \tag{A-3}$$

The series expansion of $\Psi(\mathbf{k},t)$ with respect to unperturbed wave function, Ψ_n^o gives

$$\Psi(\mathbf{k},t) = \sum_n a_n \Psi_n^0(\mathbf{k},t) \tag{A-4}$$

a_n can be obtained by substituting (A-4) into (A-3).

$$i\hbar\sum_n \frac{da_n(t)}{dt}\Psi_n^0(\mathbf{k},t) = \Delta U\Psi(\mathbf{k},t) \tag{A-5}$$

By multiplying the complex conjugate of Ψ_m^o, $\Psi_{m^*}^{o^*}$ to the both sides of above equation, the following equation is obtained.

$$i\hbar\frac{da_n(t)}{dt}\delta_{mn} = \int_{\mathbf{k}}\Psi_m^{0*}\Delta U\Psi d^3r = i\hbar\frac{da_n}{dt} \tag{A-6}$$

Here, the perturbation potential is assumed to be weak so that $\Psi(\mathbf{k},t)$ in the eq. (A-6) can be approximated to be $\Psi^0(\mathbf{k},t)$ (Born Approximation). Then eq. (A-6) becomes

$$i\hbar\frac{da_n}{dt} = \int_{\mathbf{k}} \Psi_n^{0*}(\mathbf{k},t)\Delta U\Psi^0(\mathbf{k},t)d\mathbf{k} \tag{A-7}$$

In stead of the integral notation of the above equation, the following compact notation is introduced.

$$\begin{aligned} U_{n0} &= \int \Psi_n^{0*}(\mathbf{k},t)\Delta U\Psi^0(\mathbf{k},t)d\mathbf{k} \\ &= \langle \Psi_n | \Delta U | \Psi^0 \rangle \\ &= \langle n | \Delta U | 0 \rangle \cdot \exp\left\{i\frac{E_0 - E_n}{\hbar}t\right\} \end{aligned} \tag{A-8}$$

By using above notation, the solution of eq. (A-7) can be given by

$$a_n = \frac{1}{i\hbar}\int_0^t U_{n0}\cdot\exp\left\{i\frac{E_0 - E_n}{\hbar}t\right\}dt \tag{A-9}$$

Since the perturbation potential, ΔU, of the present study is not time dependent, (A-9) can be further more simplified and

$$\begin{aligned} a_n &= \frac{U_{n0}}{i\hbar}\int_0^t \exp\left\{i\frac{E_0 - E_n}{\hbar}t\right\}dt \\ &= -\frac{U_{n0}}{\Delta E}\{e^{i\frac{\Delta E}{\hbar}t} - 1\} \end{aligned} \tag{A-10}$$

where

$$\Delta E = E_0 - E_n \tag{A-10'}$$

At time t, the probability, P_n, of finding the system at state, n, is given by

$$P_n = |a_n(t)|^2 \tag{A-11}$$

Then the substitution of (A-10) into (A-11) yields

$$P_n = |a_n(t)|^2$$

$$= \frac{\pi t}{\hbar^2}(U_{n0})^2 \frac{\sin^2 \frac{\Delta E}{2\hbar} t}{\pi t (\Delta E / 2\hbar)^2} \tag{A-12}$$

The third term of (A-12) is known as Fejer kernel [55] which provides the following δ-sequence.

$$\frac{\sin^2 \frac{\Delta E}{2\hbar} t}{\pi t (\Delta E / 2\hbar)^2} \sim \delta\left[\frac{\Delta E}{2\hbar}\right] \tag{A-13}$$

Therefore the scattering probability per unit time, Q(0, n), can be given by

$$Q(0,n) = \frac{P_n}{t}$$

$$= \frac{\pi}{\hbar^2} |\langle n | \Delta U | 0 \rangle|^2 \delta\left[\frac{\Delta E}{2\hbar}\right] \tag{A-14}$$

Appendix B. Calculation of Scattering Probability <Π> — Fourier Transformation of Perturbation Potential —

Scattering probability matrix, $S_{\mathbf{k}\mathbf{k}'}$, was given by

$$S_{\mathbf{k}\mathbf{k}'} = \langle \mathbf{k}' | \Delta U | \mathbf{k} \rangle \tag{3-41}$$

$|\mathbf{k}\rangle$ was free electron wave function and is explicitly expressed as [56]

$$|\mathbf{k}\rangle = \frac{e^{i\mathbf{k}\mathbf{r}}}{\Delta^{1/2}(2G+1)^{3/2}} \tag{B-1}$$

where Δ is the volume of the unit cell and $(2G+1)^3$ is the number of atoms in the crystal. Since constant term of ΔU can be separated as

$$\Delta U = -e\varphi(\mathbf{r}) \tag{3-35}$$

$$= -\frac{D}{\alpha} e C U_g \tag{B-2}$$

where

$$U_g = \frac{\gamma y}{x^2+(\gamma y)^2} - 2\sqrt{\alpha} K_1(\sqrt{\alpha}\,|\mathbf{r}|)\frac{\sin\vartheta}{\gamma+1} \tag{B-3}$$

attention is confined to the Fourier transformation of Ug. Let T and S be the Fourier transformation of the first term and the second term, respectively. Then,

$$T = \int_{-\infty}^{\infty}\int_{-\infty}^{\infty} e^{-i\mathbf{K}\mathbf{r}} \frac{\gamma y}{x^2+(\gamma y)^2} dx\, dy$$

$$= \left[\int_{-\infty}^{0} dx\; e^{-iK_x x} + \int_{0}^{\infty} dx\; e^{iK_x x}\right] \int_{-\infty}^{\infty} dy\; e^{-iK_y y} \frac{\gamma y}{x^2+(\gamma y)^2}$$

$$= \int_{0}^{\infty} dx\; e^{-i(-K_x)x} T_1(x) + \int_{0}^{\infty} dx\; e^{-iK_x x} T_1(x) \tag{B-4}$$

where

$$\mathbf{K} = \mathbf{k}' - \mathbf{k} \tag{B-5}$$

and

$$T_1(x) = \int_{-\infty}^{\infty} dy\; e^{-iK_y y} \frac{\gamma y}{x^2+(\gamma y)^2} \tag{B-6}$$

By putting γy to Y, above equation is transformed to

$$T_1(x) = \frac{1}{\gamma}\int_{-\infty}^{\infty} dY\, e^{-i\left|\frac{K_y}{\gamma}\right|Y}\,\frac{Y}{x^2+Y^2} \tag{B-7}$$

By the way according to Campbell [57],

$$\int_{-\infty}^{\infty}\frac{p}{p^2-\beta^2}e^{i2\pi fg}\,df = \pm\frac{1}{2}e^{-\beta|g|} \tag{B-8}$$

where

$$p = 2\pi i f \quad , \beta>0 \text{ and } \pm g>0 \tag{B-9}$$

Then comparison of eq. (B-7) with eq.(B-8) immediately gives

$$T_1(x) = \frac{1}{\gamma}\left(\pm\pi i\, e^{-2\pi x\left|-\frac{1}{2\pi}\frac{K_y}{\gamma}\right|}\right)$$

$$= \pm\frac{\pi i}{\gamma}e^{-\frac{\pi}{\gamma}|K_y|} \quad (0>\pm K_y) \tag{B-10}$$

and substitution of the eq. (B-10) into the eq. (B-4) yields

$$T = \pm\frac{\pi}{\gamma}i\left\{\int_0^{\infty} dx\, e^{-\frac{|K_y|}{\gamma}x}e^{-i(-K_x)x} + \int_0^{\infty} dx\, e^{-\frac{|K_y|}{\gamma}x}e^{-iK_x x}\right\} \tag{B-11}$$

By making use of the No. 438 of the same reference [57],

$$\int_{-\infty}^{\infty} e^{-i2\pi fg}\, e^{-\beta g}\,dg = \frac{1}{p+\beta}$$

$$= \frac{1}{i2\pi f+g} \quad (g>0) \tag{B-12}$$

comparison of eq. (B-11) with eq. (B-12) yields the following result.

$$T = \pm 2\pi i\frac{|K_y|}{(\gamma K_x)^2+K_y^2} \quad 0>\pm K_y \tag{B-13}$$

On the other hand, S is given by

$$S = \int_{-\infty}^{\infty}\int_{-\infty}^{\infty} e^{-ik_x\sqrt{a}} K_1(\sqrt{a}\,|r|)\frac{\sin\vartheta}{\gamma+1}$$

$$= \{\int_{-\infty}^{0} dy\ e^{-ik_y y} + \int_{0}^{\infty} dy\ e^{ik_y y}\}\cdot\int_{-\infty}^{\infty} dx\ e^{-ik_x x} S_1(x,y) \qquad \text{(B-3')}$$

$$= \{-\int_{0}^{\infty} dy\ e^{-i(-k_y)y} + \int_{0}^{\infty} dy\ e^{-ik_y y}\}\cdot\int_{-\infty}^{\infty} dx\ e^{-ik_x x} S_1(x,y) \qquad \text{(B-14)}$$

where coefficient 2 in the eq. (B-3) is neglected and $S_1(x,y)$ is given by

$$S_1(x,y) = \sqrt{a}\,K_1(\sqrt{a}\,|r|)\frac{\sin\vartheta}{\gamma+1}$$

$$= \frac{1}{\gamma+1}\frac{\sqrt{a}\,y}{\sqrt{x^2+y^2}} K_1(\sqrt{a}\,\sqrt{x^2+y^2}) \qquad \text{(B-15)}$$

According to No. 867 of the reference [57],

$$\int_{-\infty}^{\infty} dg\ \frac{\alpha\rho K_1[\rho(g^2+\alpha^2)^{1/2}]}{\pi(g^2+\alpha^2)^{1/2}} e^{-i2\pi fg} = \exp[-\alpha(\rho^2-p^2)^{1/2}] \qquad \text{(B-16)}$$

where

$$p = 2\pi i f \quad , \ \rho \geq \text{ and } \alpha > 0 \qquad \text{(B-17)}$$

Direct comparison between the last term of eq. (B-14) and eq. (B-16) leads the following Fourier transformation of $S_1(x,y)$.

$$\int_{-\infty}^{\infty} dx\ e^{-ik_x x} S_1(x,y) = \frac{\pi}{\gamma+1} e^{-y\sqrt{a+k_x^2}} \qquad \text{(B-18)}$$

Then, S becomes

$$S = \frac{\pi}{\gamma+1}\{-\int_{0}^{\infty} dk_y\ e^{-i(-k_y)y} e^{-y\sqrt{a+k_x^2}} + \int_{0}^{\infty} dy\ e^{-ik_y y} e^{-y\sqrt{a+k_x^2}}\} \qquad \text{(B-19)}$$

Again by making use of the No. 438 of the reference [57] given by (B-12), Fourier transformation of each term is immediately calculated.

$$S = \frac{1}{\gamma+1}\left\{-\pi\frac{1}{-iK_y+\sqrt{a+K_z^2}} + \pi\frac{1}{iK_y+\sqrt{a+K_z^2}}\right\}$$

$$= \frac{1}{\gamma+1}\frac{(-i)2\pi K_y}{K_z^2+K_y^2+a} \tag{B-20}$$

The final form of scattering probability matrix is given by

$$S_{kk'} = \pm 2\pi\cdot\frac{|K_y|}{(\gamma K_z)^2+K_y^2} + \frac{4\pi i}{\gamma+1}\frac{K_y}{K_z^2+K_y^2+a} \tag{B-21}$$

Appendix C. Numerical Evaluation of Dislocation Resistivity at $0°K$

C-1. Mathematical Basis

Mathematical basis of the numerical evaluation for a single integral equation of Fredholm type is provided in the reference [31]. Here, essential points are summarized. The following Fredholm inhomogeneous integral equation is considered.

$$\int_a^b k(x,\xi)u(\xi)d\xi - \mu u(x) = f(x) \tag{C-1}$$

In order to solve above equation numerically, interval $[a,b]$ is divided into n-equal steps, and integral is replaced by summation.

$$\int_a^b k(x,\xi)u(\xi)d\xi = \sum_{j=1}^{n} k(x,x_j)u(x_j)\frac{b-a}{n} \tag{C-2}$$

The integral equation (C-1) is attempted to be satisfied only at $x_1, x_2, \ldots, x_n$. By introducing the following notations

$$k(x_i,x_j) = k_{ij} \tag{C-3}$$

$$u(x_i) = u_i \tag{C-4}$$

and

$$f(x_i) = f_i \tag{C-5}$$

eq. (C-1) is transformed to n sets of linear algebraic equations.

$$\sum_j k_{ij} u_j \frac{b-a}{n} = \mu u_i + f_i \tag{C-6}$$

After solving these n linear inhomogeneous equations for unknown $u_1, u_2, \ldots\ldots, u_n$, a functional representation of $u(x)$ can be obtained as

$$u(x) = -\frac{f(x)}{\mu} + \frac{1}{\mu}\sum_{j=1}^{n} k(x,x_j) u_j \frac{b-a}{n} \tag{C-7}$$

C-2. Numerical Calculation of Resistivity

By applying the following relation (C-8) to the eq. 4-18

$$\mathbf{g} = (g_x, g_y, g_z)$$

$$= (h_x E_x, h_y E_y, h_z E_z) \tag{C-8}$$

the B.T.E. can be split into three equations for x, y and z components.

$$-sk_x = C \int_{\varphi'} (h_x k_x - h_x(') k_x') \ddagger k' | - e\varphi | k>_2 |^2 d\varphi'$$

$$etc. \tag{C-9}$$

etc. Since procedures are same for each component, this argument is confined to only x component. By performing the coordinate transformation given by the eqs. 3-44~3-46, above eq. (C-9) can be rewritten as

$$-e\cos\varphi = C''\int_{\varphi'}(h_x\cos\varphi - h_x(')\cos\varphi')F^e(\vartheta,\varphi,\varphi')d\varphi' \qquad \text{(C-10)}$$

where $F^e(\vartheta,\varphi,\varphi')$ is the polar coordinate representation of scattering probability matrix $|S_{kk'}|^2$ given by (B-21). On the other hand, by using (C-8), the conductivity, σ_{xx}, can be singled out from the eq. 3-58.

$$\sigma_{xx} = Ak_F\int_0^{\pi}d\vartheta\int_0^{2\pi}d\varphi h_x(\vartheta,\varphi)\sin^3\vartheta d\varphi \qquad \text{(C-11)}$$

where A was given in the eq. 3-61. Above double integral can be replaced by summation ir the following way.

$$\sigma_{xx} = Ak_F\sum_{i=1}^{M+1}\sum_{j=1}^{2M}h_x(\vartheta_i,\varphi_j)\cdot\sin^3\vartheta_i\cdot\cos^2\varphi_j\frac{\pi}{M}\frac{2\pi}{2M}$$

$$= Ak_F\sum_i\sum_j h_{ij}\cdot\sin^3\vartheta_i\cdot\cos^2\varphi_j\left\{\frac{\pi}{M}\right\}^2 \qquad \text{(C-12)}$$

where compact notation h_{ij} is introduced for $h_x(\vartheta_i,\varphi_j)$. And substitution of h, the solution of (C-10), into the eq. (C-12) yields numerical value of conductivity. This is the essential procedure.

From $F^e(\vartheta,\varphi,\varphi')$, one can single out $1/\sin^2\vartheta$ term. Then (c-10) is slightly modified to be

$$-e\ \sin^2\vartheta\cdot\cos\varphi = C''\int_{\varphi'}(h_x\cos\varphi - h_x(')\cos\varphi')F(\vartheta,\varphi,\varphi')d\varphi' \qquad \text{(C-13)}$$

On the $\vartheta_i-\varphi_k$ space, above eq. (C-13) can be rewritten as

$$-eS_i\cos\varphi_k = C''\int_0^{2\pi}(h_{ik}\cos\varphi_k - h_i(')\cos\varphi')F(\vartheta_i,\varphi_k,\varphi')d\varphi'$$

$$(i=1,2,\ldots\ldots,M+1\ ;k=1,2,\ldots\ldots,2M+1) \qquad \text{(C-14)}$$

where

$$S_i = \sin^2\vartheta_i \tag{C-15}$$

By applying the Trapezoidal rule to the eq. (C-14), integral can be replace by summation in the following form.

$$-eS_i\cos\varphi_k = C'\left\{\sum_{j=2}^{2M}(h_{ik}\cos\varphi_k - h_{ij}\cos\varphi_j)F_{ik}^j\frac{2\pi}{2M}\right.$$

$$+\frac{1}{2}(h_{ik}\cos\varphi_k - h_{i1}\cos\varphi_1)F_{ik}^1\frac{2\pi}{2M}$$

$$\left.+\frac{1}{2}(h_{ik}\cos\varphi_k - h_{i\,2M+1}\cos\varphi_{2M+1})F_{ik}^{2M+1}\frac{2\pi}{2M}\right\}$$

$$(i=1,2,\ldots\ldots,M+1;k,j=1,2,\ldots\ldots,2M+1) \tag{C-16}$$

where F_{ik}^j is the compact notatio. of $F(\vartheta_i,\varphi_k,\varphi_j')$. Then, for each (i,k), $2M+1$ sets of linear algebraic equations for unknown h_{ij} is set up. Now, let us define new tensor, H_{ij}.

$$H_{ij} = h_{ij}\cos\varphi_j \tag{C-17}$$

Then eq. (C-16) is transformed to

$$\sum_{j=2}^{2M}(H_{ij}-H_{ik})F_{ik}^j+\frac{1}{2}(H_{i1}-H_{ik})F_{ik}^1+\frac{1}{2}(H_{i\,2M+1}-H_{ik})F_{ik}^{2M+1} = \frac{e}{C'}S_i\cos\varphi_k \tag{C-18}$$

By making use of the next relations (C-19)~(C-21) which are easily verified,

$$h_{i1} = h_{i\,2M+1} \tag{C-19}$$

$$F_{i1}^j = F_{i\,2M+1}^j \tag{C-20}$$

$$F_{ik}^1 = F_{ik}^{2M+1}, \tag{C-21}$$

$2M+1$ sets of equations can be reduced to $2M$ sets of equations. And the following matrix notation of (C-18) is introduced.

$$\begin{bmatrix} -(F_{11}^2+F_{11}^3+.....+F_{11}^{2M}) & F_{11}^2 & F_{11}^3 & . . & F_{11}^{2M} \\ F_{12}^1 & -(F_{12}^1+F_{12}^3+.....+F_{12}^{2M}) & F_{12}^3 & . . & F_{12}^{2M} \\ . & . & -(F_{13}^1+F_{13}^2+F_{13}^4+.....+F_{13}^{2M}) & . . & . \\ . & . & . & . . & . \\ . & . & . & . . & . \\ F_{1\,2M}^1 & F_{1\,2M}^2 & F_{1\,2M}^3 & . . & -(F_{1\,2M}^1+F_{1\,2M}^2+.....+F_{1\,2M}^{2M-1}) \end{bmatrix}$$

$$\cdot \begin{bmatrix} H_{i1} \\ H_{i2} \\ . \\ . \\ . \\ H_{i\,2M} \end{bmatrix}$$

$$= \frac{a}{C''} S_i \begin{bmatrix} \cos\varphi_1 \\ \cos\varphi_2 \\ . \\ . \\ \cos\varphi_{2M} \end{bmatrix} \qquad \text{(C-22)}$$

Then for each ϑ_i, $2M$ sets of H_{ik} value, i.e. h_{ik}, is numerically evaluated. This procedure is repeated M times for $\vartheta_1,\vartheta_2,.....,\vartheta_i,.....,\vartheta_M$, and by substituting the results into the eq. (C-12), one can obtain conductivity σ_{zz}, and therefore, dislocation resistivity ρ_z

$$\rho_z^{(num)} = \frac{1}{\sigma_{zz}^{(num)}}$$

$$= \frac{1}{Ak_F} \frac{1}{\sum_i \sum_j h_{ij} \sin^3\vartheta_i \cdot \cos^2\varphi_j \left(\frac{\pi}{M}\right)^2} \qquad \text{(C-23)}$$

Appendix D. Modification for a Poly Crystal

Although the final product of the modification of electrical resistivity for a poly crystal is given in the reference [56], the derivation is not provided. In this appendix, the general derivation of the average resistivity of a poly crystal is carried out. Components of the resistivity tensor, Ω_{kl}, and unit vector n_j in a

certain direction shown in the Fig.21 are given by

$$\{\Omega_{kl}\} = \begin{bmatrix} \rho_x & 0 & 0 \\ 0 & \rho_y & 0 \\ 0 & 0 & 0 \end{bmatrix} \tag{D-1}$$

and

$$\{n_j\} = \begin{Bmatrix} \sin\alpha\cdot\cos\beta \\ \sin\alpha\cdot\sin\beta \\ \cos\alpha \end{Bmatrix} \tag{D-2}$$

Then the components of the resistivity, $\rho_i^{\alpha\beta}$, in the x, y and z direction is obtained as

$$\rho_i^{\alpha\beta} = \Omega_{kl} n_l$$

$$= \begin{Bmatrix} \rho_x\cdot\sin\alpha\cdot\cos\beta \\ \rho_y\cdot\sin\alpha\cdot\sin\beta \\ 0 \end{Bmatrix} \tag{D-3}$$

Since the measurement is carried out on a normal plane to $\vec{n}$, the component of resistivity along $\vec{n}$ should be calculated.

$$\rho_n^{\alpha\beta} = \rho_k^{\alpha\beta} n_k$$

$$= \sin^2\alpha(\rho_x\cos^2\alpha + \rho_y\sin^2\beta) \tag{D-4}$$

By considering the fact that the solid angle at (α,β) is given by

$$d\omega = \sin\alpha\cdot d\alpha\cdot d\beta \tag{D-5}$$

the average resistivity is calculated in the following integral.

$$\int_0^{\pi/2} d\alpha \int_0^{2\pi} d\beta \frac{d\omega}{2\pi} \rho_{\alpha\beta} = \frac{1}{2}\int_0^{\pi/2} d\alpha \int_0^{2\pi} d\beta\, \rho_n^{\alpha\beta}$$

$$= \frac{1}{3}(\rho_x + \rho_y)$$

$$= \frac{4}{3}\rho_x \qquad \text{(D-6)}$$

FIGURE CAPTIONS

Figure 1. Definition of two types of coordinate systems for the description of edge dislocation motion.

Figure 2. Numerical evaluation of the third term appearing in eq. 3-16 and comparisons of its magnitude with the other two terms. Comparisons are carried out along the diagonal direction in a coordinate. $v=0.25\,v_t$ and $\sqrt{\alpha}$ $1.5\times10^6\,[cm^{-1}]$

Figure 3. Same as Figure 2, but employed velocity is $v=0.5v_t$ and $\sqrt{\alpha}=1.5\times10^6$ $[cm^{-1}]$

Figure 4. Same as Figures 2 and 3, but comparisons are carried out along a circle of radius, 3b.

Figure 5. Configurational relations between Cartesian and Polar coordinates in k-space.

Figure 6. A model crystal in which an edge dislocation motion with constant velocity is characterized.

Figure 7. Deviations of electron densities from those in a dislocation free state. contributions of the first term in the eq. 4-10 are compared in terms of dislocation velocity. GM and SCR stands for $\gamma=\frac{v}{v_t}$ and $\sqrt{\alpha'}$, respectively. The darker colors indicate higher electron densities. The first term is independent of the screening constant.

Figure 8. Contributions of the second term and whole term in eq. 4-10 are compared in terms of dislocation velocity for a constant screening constant, $\sqrt{\alpha'}=1.0$.

Figure 9. Comparisons for a constant screening constant, $\sqrt{\alpha'}=1.5$.

Figure 10. Comparisons for a constant screening constant, $\sqrt{\alpha'}=2.0$.

Figure 11. Schematic picture of the employed perturbation potential eq. 3-18 for the case of $\frac{v}{v_t}=0.5$ and $\sqrt{\alpha}=1.0\times10^8\,[cm^{-1}]$

Figure 12. Contribution of the first term in the eq. 3-18.

Figure 13. Contributions of the second term, the screening term

Figure 14. Dependencies of the force factor F^* in the eq. 3-90 on the normalized velocities for four kinds of Fermi vector. unit is arbitrary.

Figure 15. Magnified graph of Figure 14 for normalized velocities less than 0.01. Unit is same as Figure 14.

Figure 16. Dependencies of Resistivities on normalized velocities for nine kinds of Fermi vector.

Figure 17. Geometrical distribution of magnetic induction calculated numerically for the case of $\frac{v}{v_t}=0.3$. Values in the figure are normalized by constant terms in the eq. 3-98.

Figure 18. Dependencies of magnetic induction on y-coordinates at fixed x coordinate, $x=5b$ for three types of velocities.

Figure 19. A model which describes collective behavior of dislocations.

Figure 20. Magnified view of force balance condition on a dislocation interacting with point obstacles.

Figure 21. Relations among coordinates appearing in APPENDIX D.

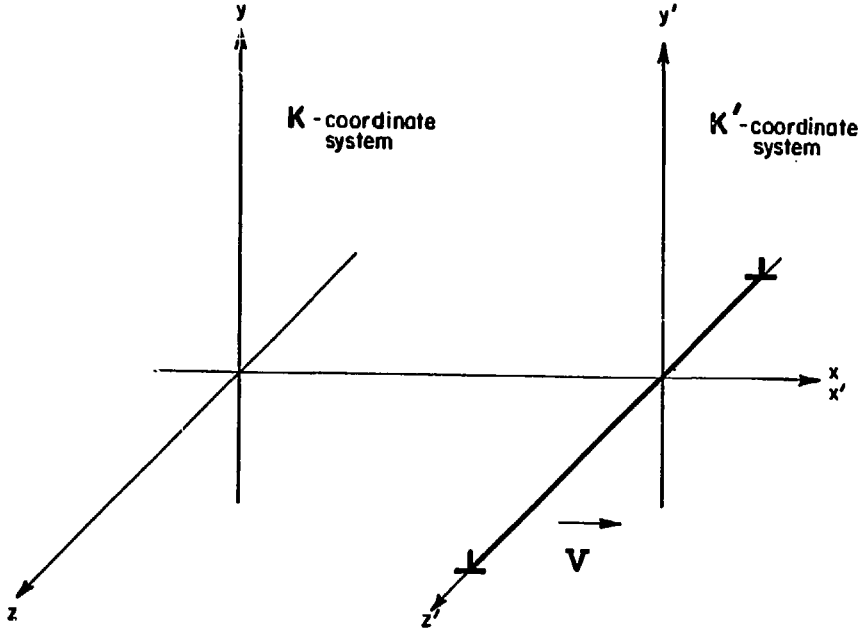

XBL821I-6805

Figure 1

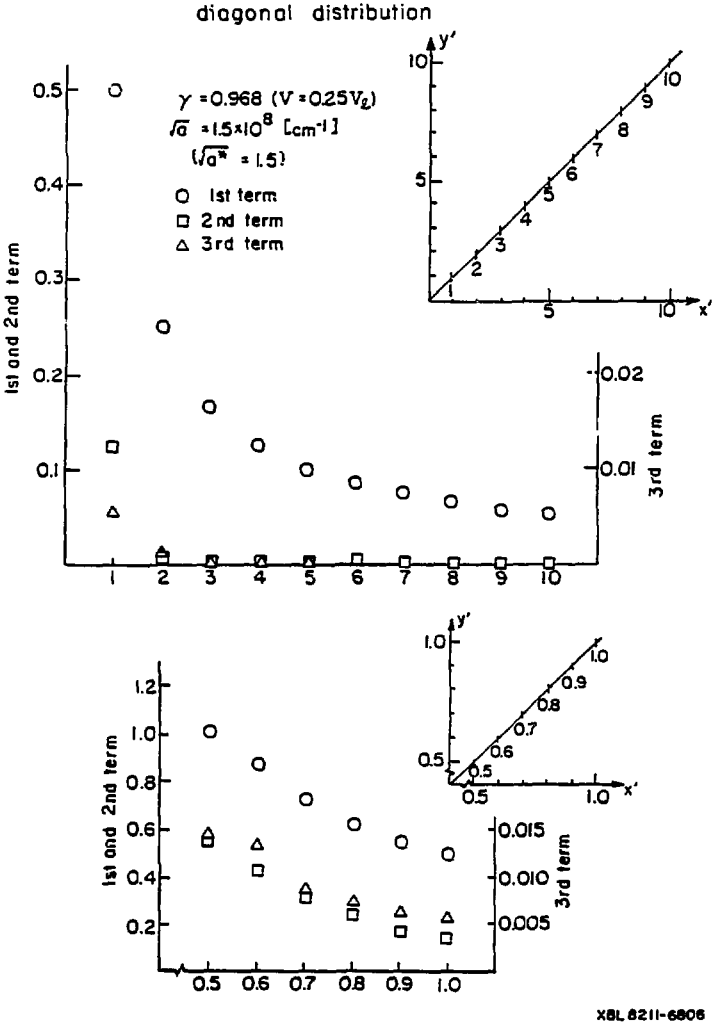
diagonal distribution
γ = 0.968 (V = 0.25 V_g)
√a = 1.5×10^8 [cm^-1]
(√a* = 1.5)
○ 1st term
□ 2nd term
△ 3rd term
1st and 2nd term
3rd term
y'
x'
1st and 2nd term
3rd term
y'
x'
XBL 8211-6806

Figure 2

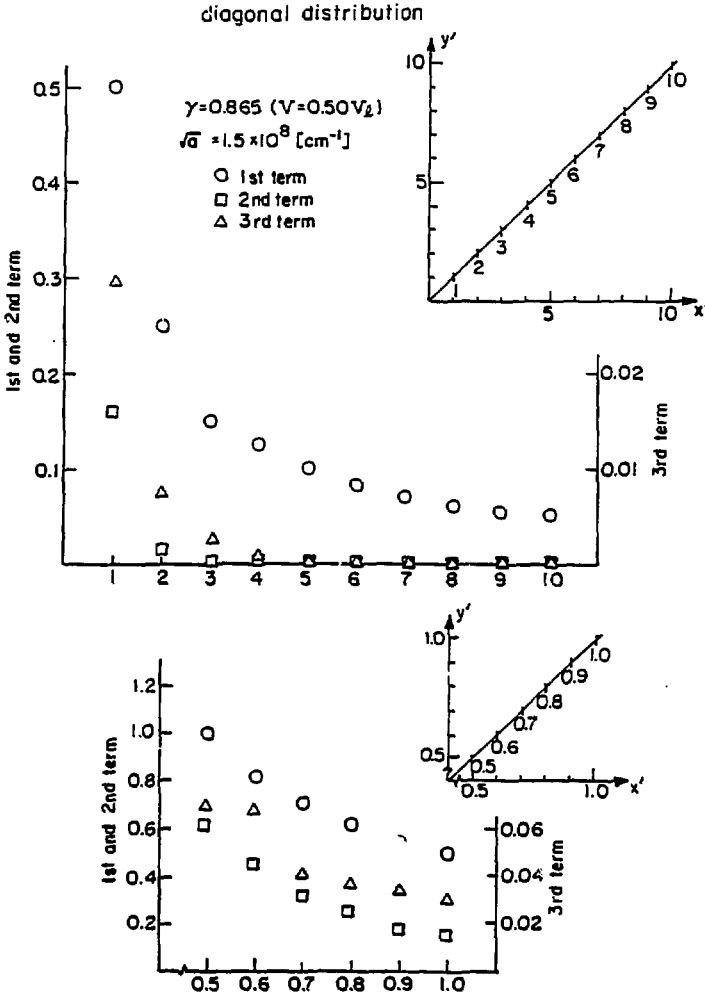
diagonal distribution
γ=0.865 (V=0.50V₂)
√a =1.5×10⁸ [cm⁻¹]
○ 1st term
□ 2nd term
△ 3rd term
1st and 2nd term
3rd term
y'
x'
1st and 2nd term
3rd term
y'
x'
XBL 8211-6807

Figure 3

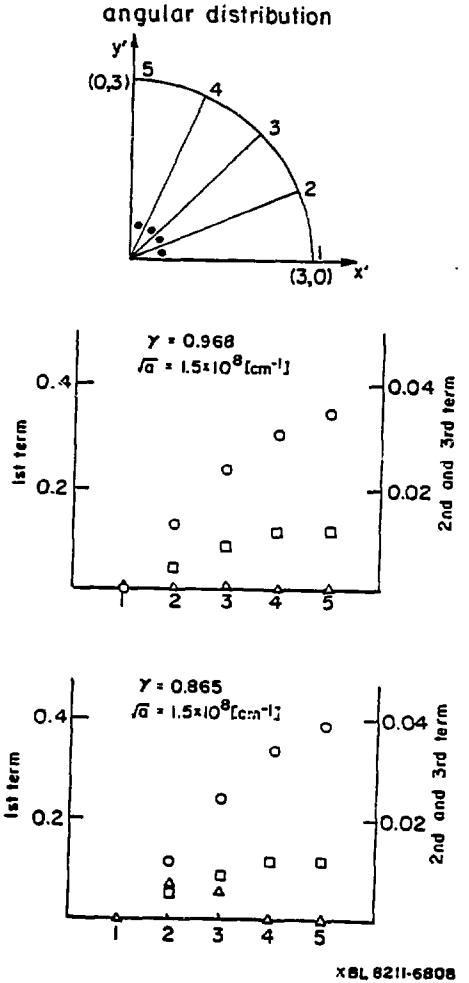
angular distribution
y'
5
(0,3)
4
3
2
1
(3,0)
x'
γ = 0.968
√a = 1.5×10⁸[cm⁻¹]
0.4
0.2
1st term
0.04
0.02
2nd and 3rd term
1
2
3
4
5
γ = 0.865
√a = 1.5×10⁸[cm⁻¹]
0.4
0.2
1st term
0.04
0.02
2nd and 3rd term
1
2
3
4
5
XBL 8211-6808

Figure 4

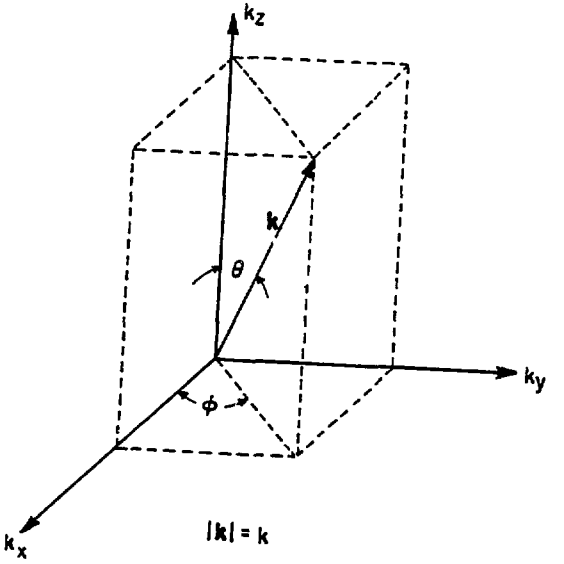

XBL 8211-6809

Figure 5

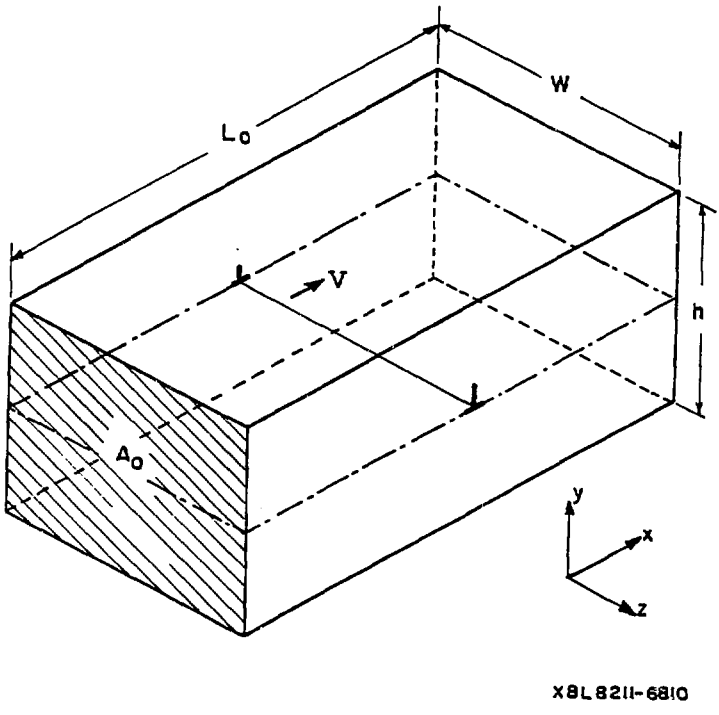

Figure 6

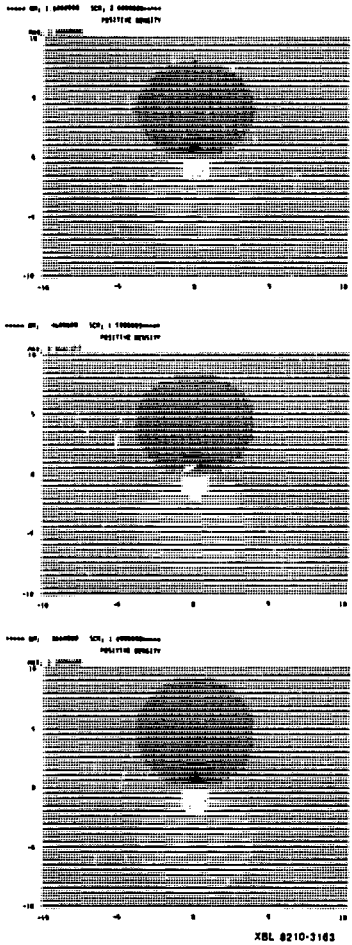

XBL 8210-3163

Figure 7

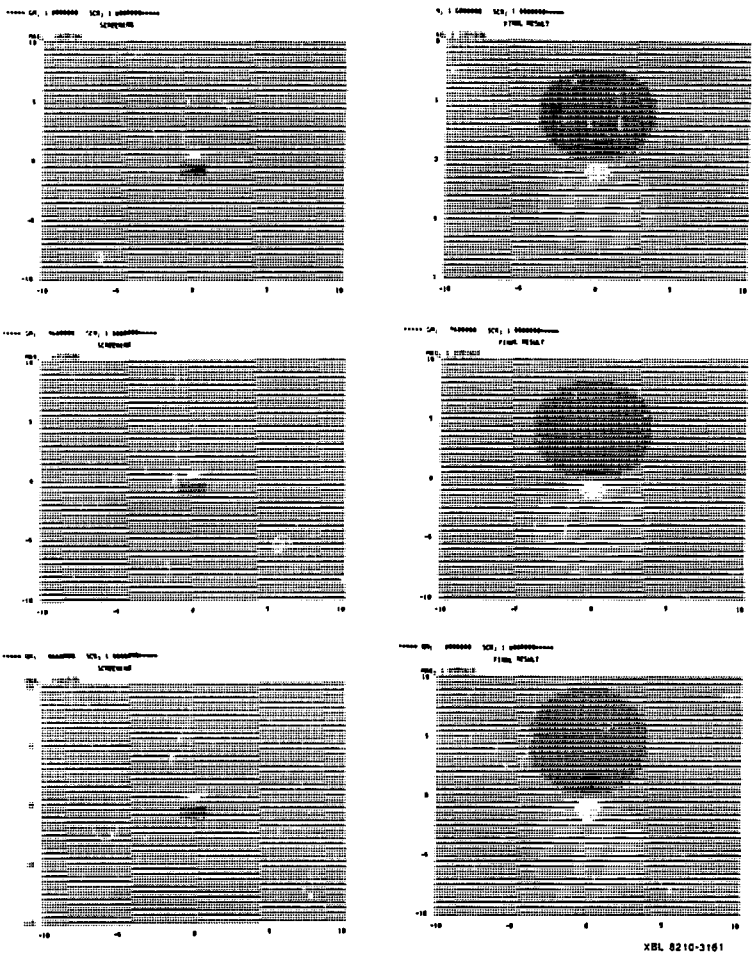

XBL 8210-3161

Figure 8

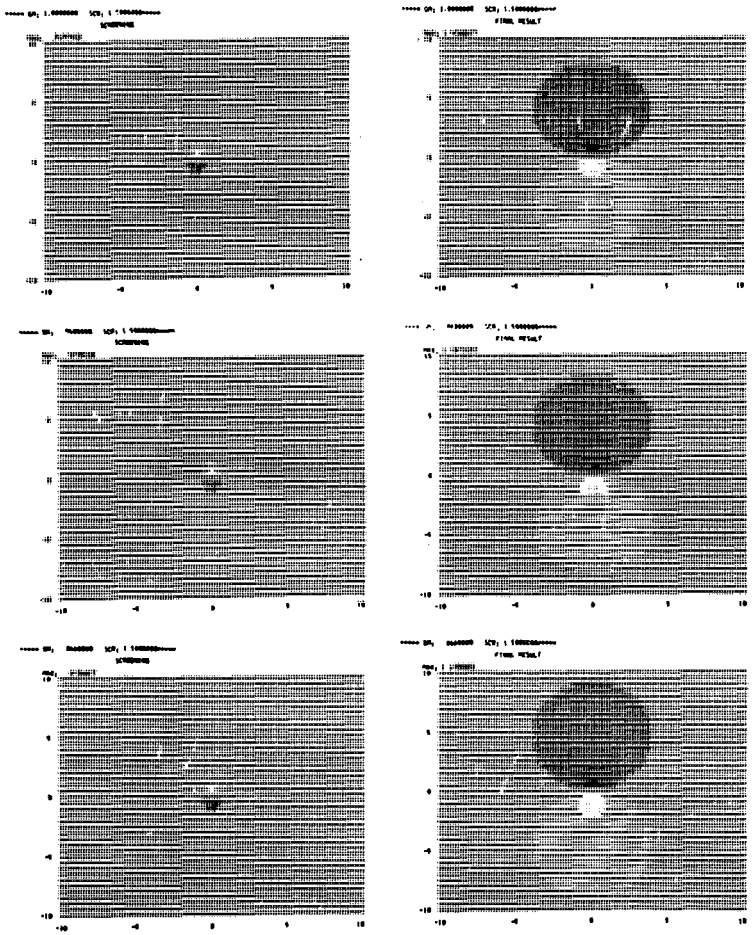

XBL 8210-3160

Figure 9

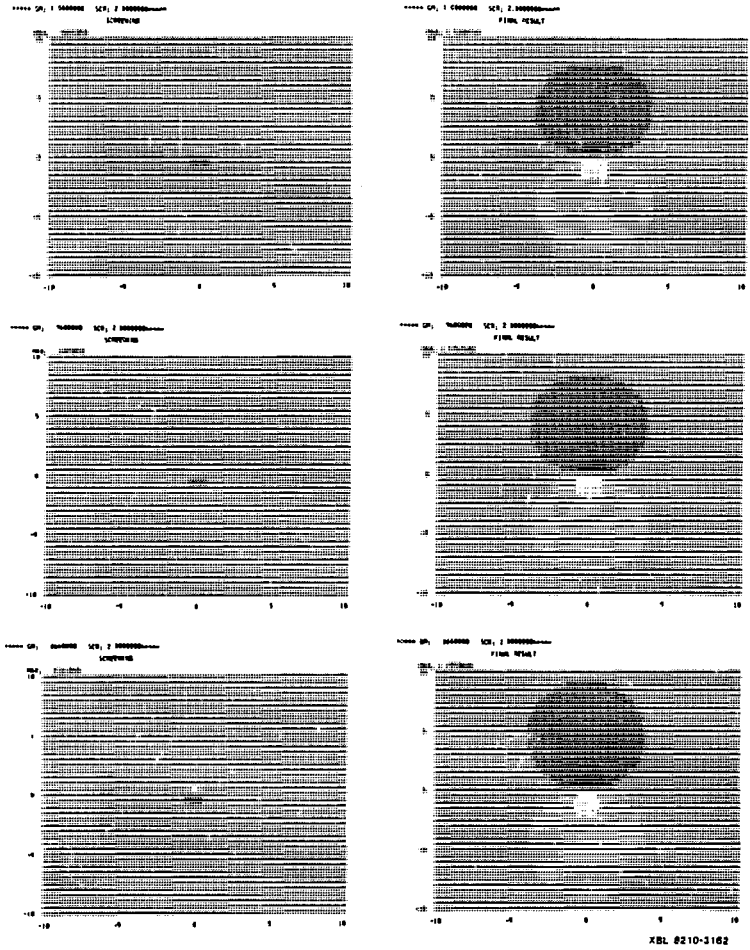

XBL 8210-3162

Figure 10

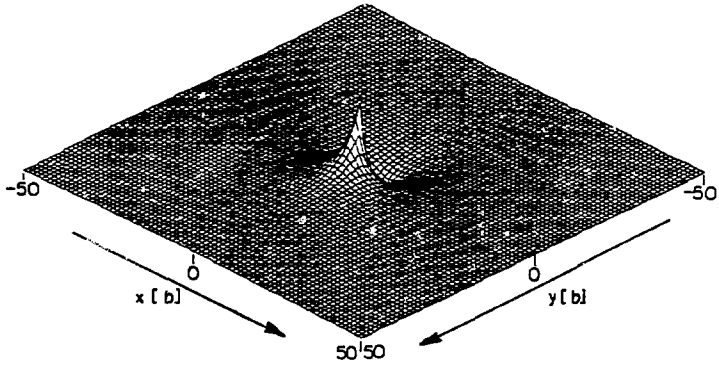

PERTURBATION POTENTIAL

$\gamma = 0.86$

$\sqrt{a} = 1.0 \times 10^8\ [cm^{-1}]$

XBL 8211-6819

Figure 11

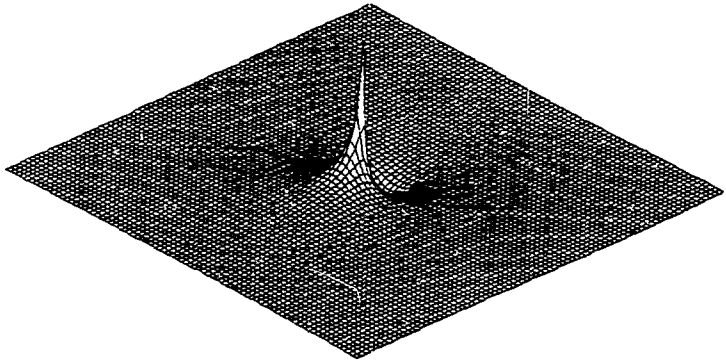

1ST TERM
(positive charge)

XBL8211-6820

Figure 12

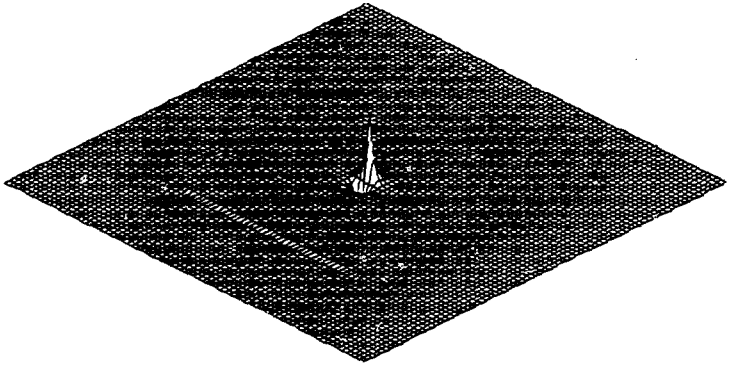

2ND TERM
(screening contribution)

XBL 8211-6821

Figure 13

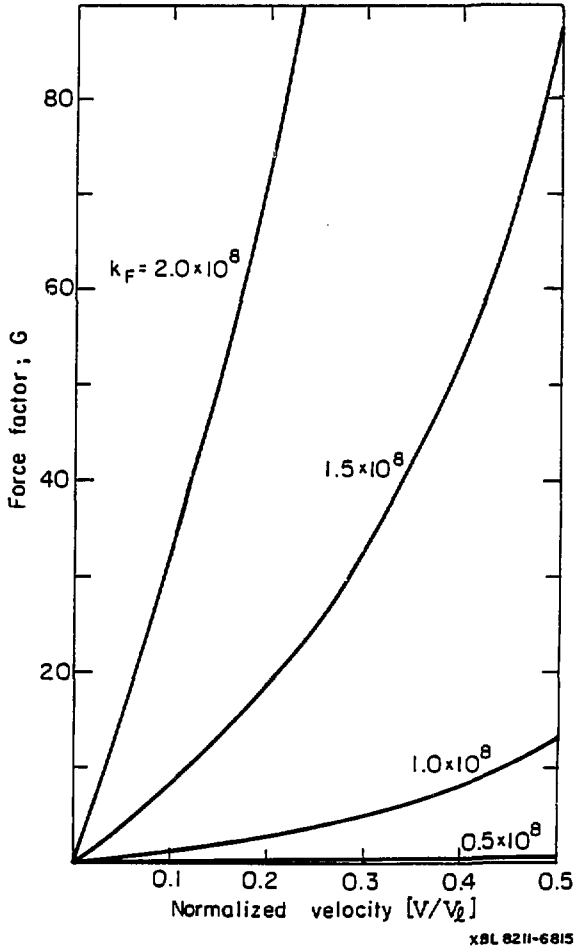
80
60
40
20
Force factor; G
$k_F = 2.0 \times 10^8$
1.5×10^8
1.0×10^8
0.5×10^8
0.1
0.2
0.3
0.4
0.5
Normalized velocity [V/V$_\ell$]
XBL 8211-6815

Figure 14

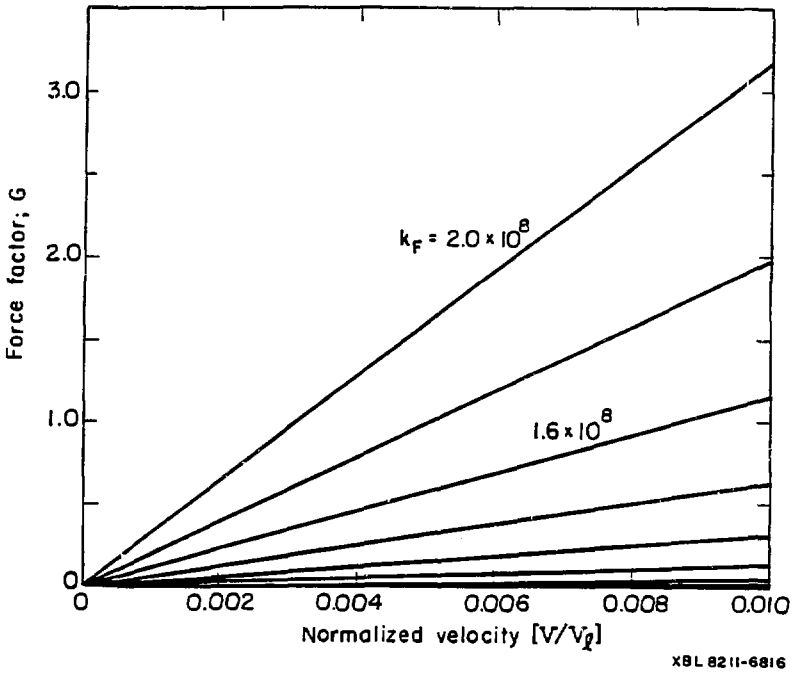
3.0
2.0
1.0
0
Force factor; G
$k_F = 2.0 \times 10^8$
1.6×10^8
0
0.002
0.004
0.006
0.008
0.010
Normalized velocity [V/V_0]
XBL 8211-6816

Figure 15

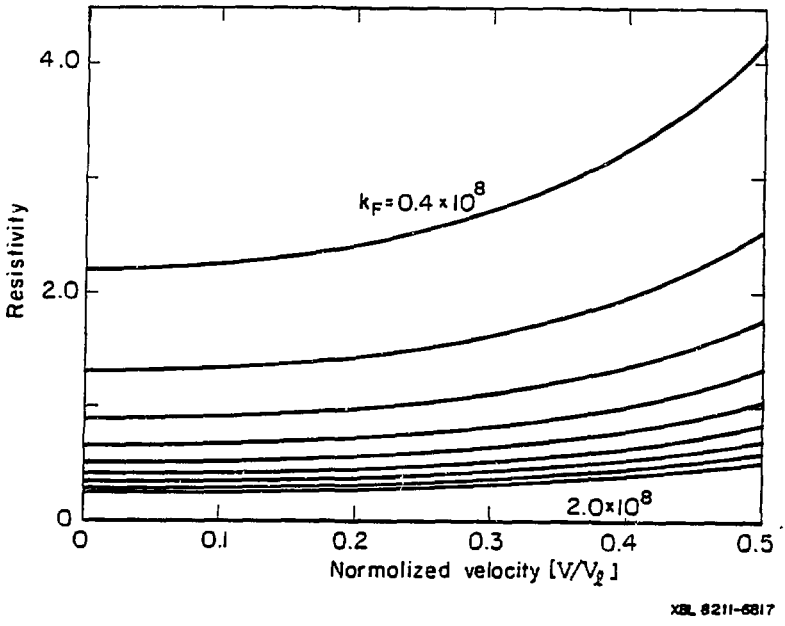
4.0
2.0
0
Resistivity
$k_F = 0.4 \times 10^8$
2.0×10^8
0
0.1
0.2
0.3
0.4
0.5
Normolized velocity [V/V_ℓ]
XBL 8211-6817

Figure 16

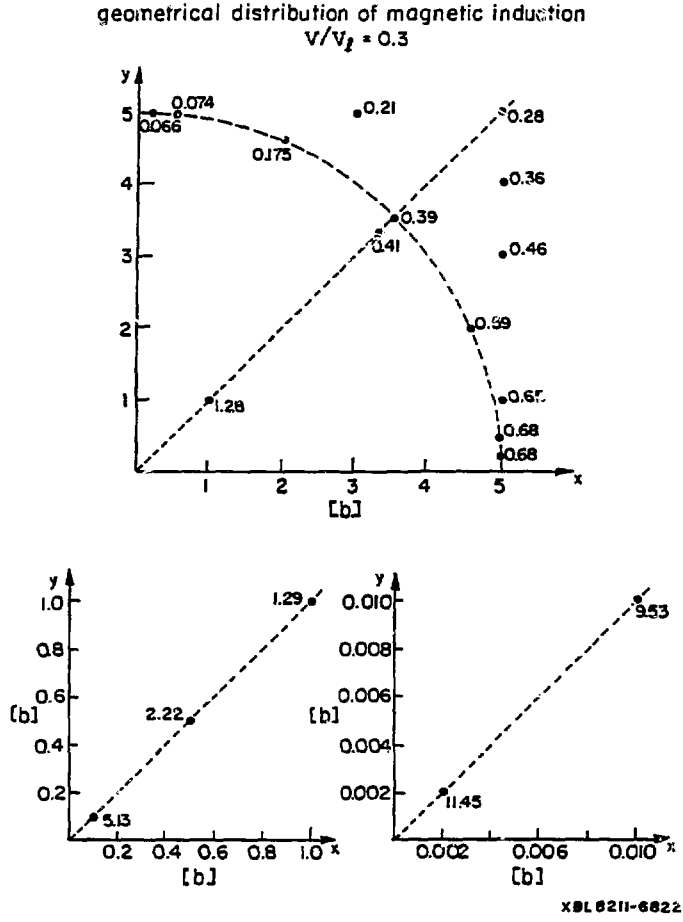
geometrical distribution of magnetic induction
V/V_ℓ = 0.3
y
x
[b]
0.074
0.066
0.175
0.21
0.28
0.36
0.39
0.41
0.46
0.59
0.67
0.68
0.68
1.28
1.29
2.22
5.13
9.53
11.45
XBL 8211-6822

Figure 17

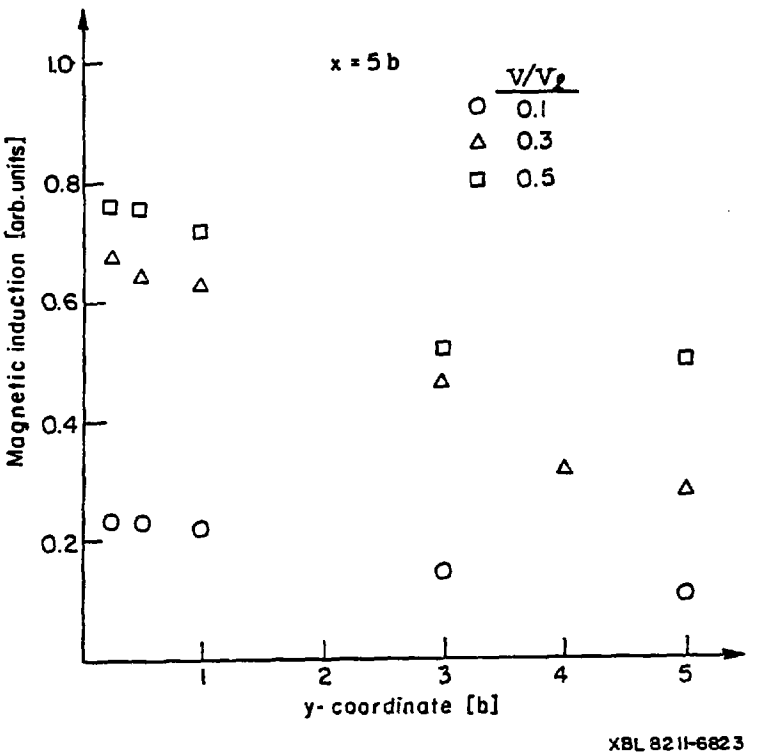
x = 5 b
V/V₀
0.1
0.3
0.5
Magnetic induction [arb. units]
1.0
0.8
0.6
0.4
0.2
1
2
3
4
5
y- coordinate [b]
XBL 8211-6823

Figure 18

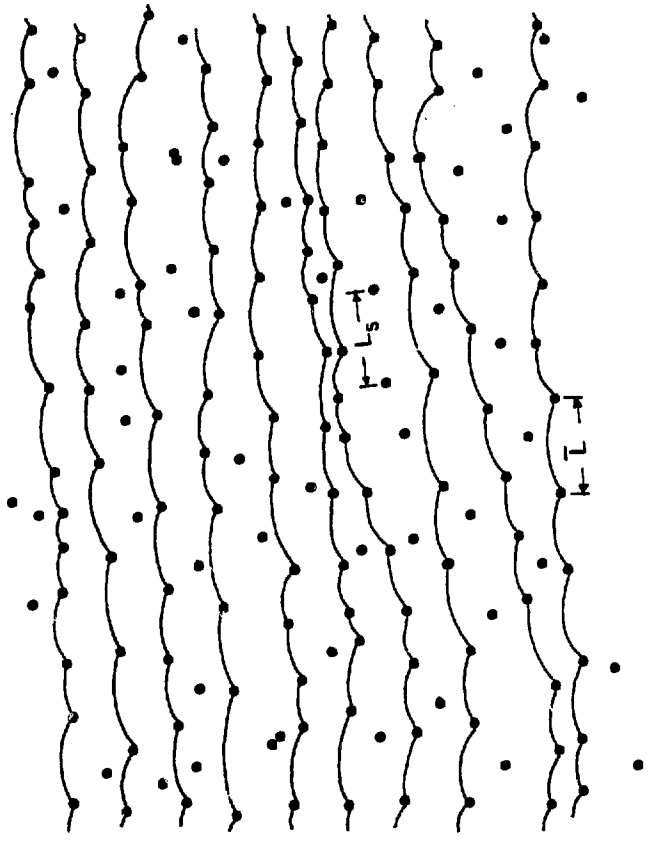

Figure 19

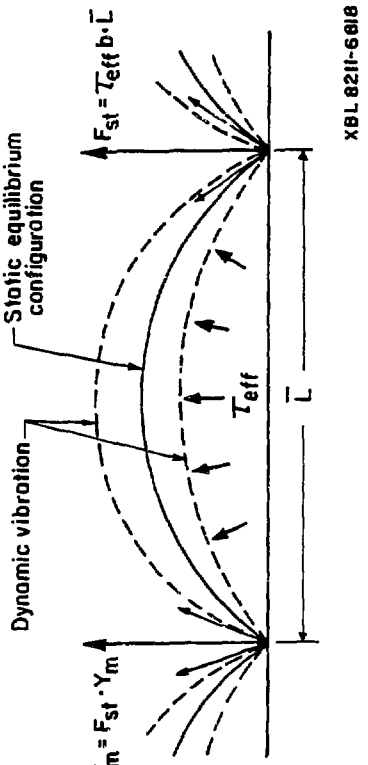
Static equilibrium configuration
Dynamic vibration
$F_{st} = \tau_{eff} b \cdot \bar{L}$
$F_m = F_{st} \cdot Y_m$
τ_{eff}
$\bar{L}$
XBL 8211-6818

Figure 20

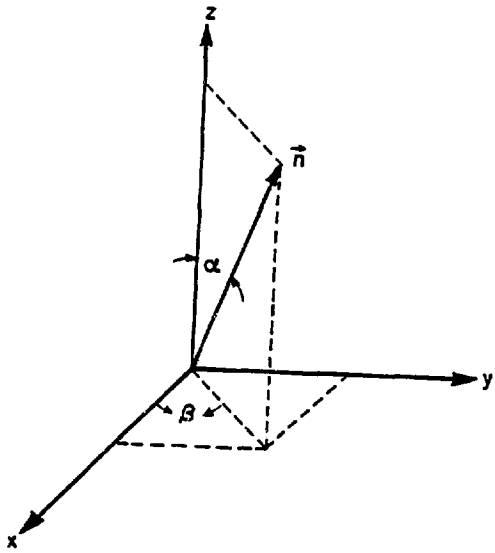

XBL8211-6813

Figure 21

LIST OF TABLES

	Numerical	Analytical
ρ_x	0.615 ± 0.10	0.648
ρ_y	1.36 ± 0.01	1.943
ρ_z	$(1.01 \pm 0.13)\ 10^{-10}$	0

XBL8211-6812

Table 1

	Al	Cu	Pb
b burgers vector	2.86 [Å]	2.56	3.50
k_F Fermi vector	1.75 $\times 10^8$ [cm^{-1}]	1.36 $\times 10^8$	1.57 $\times 10^8$
V_s/V_l	0.474	0.453	0.352
m mass of electron	9.1×10^{-28} [g]		
$\hbar$ Planck's constant	1.1×10^{-27} [erg-sec]		
e elementary charge	4.8×10^{-10} [esu]		

XBL 8211-6814

Table 2

	Author	Al	Cu	Pb	Ref.
Experimental	Hikata Elbaum			8.65×10^{-5}	58
	Victoria, Dharan, Hauser Dorn	2.45×10^{-4} ~ 3.6×10^{-4}			59
	Hikata, Johnson, Elbaum	1.37×10^{-5}			37
Theoretical	Mason			$\sim10^{-2}$	15
	Holstein	2.72×10^{-4}	8.78×10^{-5}	2.18×10^{-4}	18
	Brailsford	6.59×10^{-6}	1.59×10^{-6}	1.67×10^{-6}	21
	Present Study	3.63×10^{-6}	7.62×10^{-7}	1.00×10^{-6}	

unit; dyn-sec/cm^2

XBL8211-6811

Table 3

REFERENCES

1. A. Ewing and W. Rosenhain: Phil. Trans. Roy. Soc., A193 (1899) 353 *It is reported that O. Mugge had already suggested the existence of a dislocation in 1883.
2. H. Kojima and T. Suzuki: Phys. Rev. Letters, 21 (1968) 896
3. V. V. Pustovalov, V. I. Startsev, D. A. Didenko and V. S. Vermenko: Sov. Phys. Solid State, 11 (1969) 1119
4. K. Kamada and I. Yoshizawa: J. Phys. Soc. Japan, 31 (1971) 1056
5. K. Marukawa: J. Phys. Soc. Japan, 22 (1967) 499
6. J. S. Koehler: Imperfections in Nearly Perfect Crystals (John Wiley and Sons, Inc., New York, 1952), 197
7. W. P. Mason: J. Acoust. Soc. Amer., 32 (1960) 458
8. V. P. Soldatov, V. I. Startsev and T. I. Vainblat: phys. stat. sol. 37 (1970) 47
9. V. I. Startsev, V. P. Soldatov, V. D. Natsik and V. V. Abraimov: phys. stat. sol. (a) 59 (1980) 377
10. M. Suenaga and J. M. Galligan: Script. Met. 5 (1971) 63
11. J. M. Galligan, T. H. Lin and C. S. Pang: Phys. Rev. Letters, 38 (1977) 405, J. M. Galligan and C. S. Pang: J. Appl. Phys. 50 (1979) 6253
12. F. Iida, T. Suzuki, E. Kramoto and S. Takeuchi: Tech. Rep. ISSP, Ser. A, (1978) No. 900
13. G. P. Huffman and N. Louat: Phys. Rev. Letters, 24 (1970) 1055
14. V. G. BAR'YAKHTAR, YE. I. DRUINSKIY and I. I. FAL'KO: Phys. Metals and Metallography 33 (1972) 1
15. W. P. Mason: Appl. Phys. Letters, 6 (1965) 111

16. W. P. Mason: Phys. Rev., 143 (1966) 229

17. B. R. Tittmann and H. E. Bommel, Phys. Rev., 151 (1966) 178

18. T. Holstein (see APPENDIX to Ref. 17)

19. G. P. Huffman and N. P. Louat: Phys. Rev. Letters, 19 (1967) 518

20. G. P. Huffman and N. Louat: Phys. Rev., 176 (1968) 773

21. A. D. Brailsford: Phys. Rev., 186 (1969) 959

22. M. H. Cohen and M. J. Harrison: Phys. Rev., 117 (1960) 937

23. J. M. Ziman: Principles of the Theory of Solids (CAMBRIDGE UNIV. PRESS, 1972), chapt. 7.

24. J. D. Jackson: CLASSICAL ELECTRODYNAMICS (John Wiley and Sons, Inc., New York, (1963)), chapt. 11

25. K. Sumino: Bull. Japan Inst. Metals, 10 (1971) 693

26. A. H. Cottrell, S. C. Hunter and F. R. N. Nabarro: Phil. Mag., 44 (1953) 1064

27. Arfken: Mathematical Method for Physicists (Academic Press), 760

28. W. J. Moore: PHYSICAL CHEMISTRY (Prentice-Hall, Inc., 1962), chapt. 14

29. J. M. Ziman (see section 7-1 to Ref. 23)

30. for example C. Kettel: Introduction to Solid State Physics (John Wiley and Sons, Inc. 1976) 5th ed., chapt. 5

31. I. Stakgold: GREEN'S FUNCTIONS AND BOUNDARY VALUE PROBLEMS (John Wiley and Sons, Inc., New York, 1979), chapt. 6

32. A. Matthiessen and C. Vogt: Ann Phys., Lpzg., 122 (1864) 19

33. for example C. Kittel (see chapt. 6 to Ref. 30)

34. V. Vitek: Phil. Mag., 21 (1970) 1275; Crystal Lattice Defects, 5 (1974) 1

35. J. Th. M. De Hosson: Int. J. Quantum Chemistry, 18 (1980) 575

36. J. M. Ziman (see section 4-5 to Ref. 23)

37. A. Hikata, R. A. Johnson and C. Elbaum: Phys. Rev. Letters, 24 (1970) 215

38. Z. S. Basinski, J. S. Dugdale and A. Howie: Phil. Mag., 8 (1963) 1989

39. J. Bass: Adv. Phys., 91 (1972) 431

40. J. G. Rider and C. T. B. Foxon: Phil. Mag., 13 (1966) 289

41. for example C. Kittel (see chapt. 14 to Ref. 30)

42. J. J. Gilman and W. G. Johnston (Seitz and Turnbull ed., Solid State Physics 13, Academic Press 1962) 147, W. G. Johnston: J. Appl. Phys., 33 (1962) 2716

43. H. Alexander and P. Haasen: Solid. State Physics, 22 (1968) 28

44. I. Yonezawa and K. Sumino: phys. stat. sol. (a), 50 (1978) 685

45. M. Suezawa, K. Sumino and I. Yonezawa: phys. stat. sol. (a). 51 (1979) 217

46. K. Sumino, S. Kodaka and K. Kojima: Mater. Sci. Eng., 13 (1974) 263

47. K. Nishioka and K. Ohsaka: Phil. Mag. A, 37 (1978) 561 48., K. Sumino: Bull. Jap. Inst. Metals, 10 (1971) 761

49. J. J. Gilman: J. Appl. Phys., 39 (1968) 6086, E. Kuramoto, Y. Aono, K. Kitajima: Bull. Jap. Inst. Metals, 19 (1980) 348

50. J. Friedel: Dislocations (ADDISON-WESLEY PUBLISHING COMPANY, Inc., Mass., 1967)

51. A. V Granato: Phys. Rev. Letters, 27 (1971) 660; Phys. Rev.,B4 (1971) 2196 (see also Ref. 12)

52. R. D. Isaac and A. V. Granato: (Proceed. 5th Int. Conf. Strength of Metals and Alloys, Aachen, W. Germany 1979) 493

53. S. Altintas: Ph.D Thesis, University of California, Berkely, 1978

54. K. Hanson and J. W. Morris, Jr.: J. Appl. Phys., 46 (1975) 2678

55. I. Stakgold (see chapt. 2 to Ref. 31)

56. J. K. Mackenzie and E. H. Sondheimer: Phys. Rev. 77 (1950) 264

57. G. Campbell and R. M. Foster: Fourier Integrals(D. VAN NOSTRAND COMPANY, INC.) No. 445

58. A. Hikata and C. Elbaum: Phys. Rev. Letters, 18 (1967) 750

59. M. P. Victoria, C. K. H. Dharan, F. E. Hauser and J. E. Dorn: J. Appl. Phys., 41 (1970) 674

60. T. Ninomiya: Bull. Jap. Inst. Metals, 12 (1973) 469

This report was done with support from the Department of Energy. Any conclusions or opinions expressed in this report represent solely those of the author(s) and not necessarily those of The Regents of the University of California, the Lawrence Berkeley Laboratory or the Department of Energy.

Reference to a company or product name does not imply approval or recommendation of the product by the University of California or the U.S. Department of Energy to the exclusion of others that may be suitable.